


RESEARCH ARTICLE

Open Access



Tumor microenvironment modulation enhances immunologic benefit of chemoradiotherapy

Aurelie Hanoteau^{1*} , Jared M. Newton^{1,2}, Rosemarie Krupar³, Chen Huang^{4,5}, Hsuan-Chen Liu^{1,2}, Angelina Gaspero¹, Robyn D. Gartrell⁶, Yvonne M. Saenger⁷, Thomas D. Hart⁷, Saskia J. Santegoets⁸, Damya Laoui^{9,10}, Chad Spanos¹¹, Falguni Parikh¹, Padmini Jayaraman¹, Bing Zhang^{4,5}, Sjoerd H. Van der Burg⁸, Jo A. Van Ginderachter^{9,10}, Cornelis J. M. Melief¹² and Andrew G. Sikora^{1,13*}

Abstract

Background: Chemoradiotherapy (CRT) remains one of the most common cancer treatment modalities, and recent data suggest that CRT is maximally effective when there is generation of an anti-tumoral immune response. However, CRT has also been shown to promote immunosuppressive mechanisms which must be blocked or reversed to maximize its immune stimulating effects.

Methods: Therefore, using a preclinical model of human papillomavirus (HPV)-associated head and neck squamous cell carcinoma (HNSCC), we developed a clinically relevant therapy combining CRT and two existing immunomodulatory drugs: cyclophosphamide (CTX) and the small molecule inducible nitric oxide synthase (iNOS) inhibitor L-n6-(1-iminoethyl)-lysine (L-NIL). In this model, we treated the syngeneic HPV-HNSCC mEER tumor-bearing mice with fractionated (10 fractions of 3 Gy) tumor-directed radiation and weekly cisplatin administration. We compared the immune responses induced by CRT and those induced by combinatory treatment (CRT + CTX/L-NIL) with flow cytometry, quantitative multiplex immunofluorescence and by profiling immune-related gene expression changes.

Results: We show that combination treatment favorably remodels the tumor myeloid immune microenvironment including an increase in anti-tumor immune cell types (inflammatory monocytes and M1-like macrophages) and a decrease in immunosuppressive granulocytic myeloid-derived suppressor cells (MDSCs). Intratumoral T cell infiltration and tumor antigen specificity of T cells were also improved, including a 31.8-fold increase in the CD8⁺ T cell/ regulatory T cell ratio and a significant increase in tumor antigen-specific CD8⁺ T cells compared to CRT alone. CTX/LNIL immunomodulation was also shown to significantly improve CRT efficacy, leading to rejection of 21% established tumors in a CD8-dependent manner.

Conclusions: Overall, these data show that modulation of the tumor immune microenvironment with CTX/L-NIL enhances susceptibility of treatment-refractory tumors to CRT. The combination of tumor immune microenvironment modulation with CRT constitutes a translationally relevant approach to enhance CRT efficacy through enhanced immune activation.

Keywords: Immunotherapy, Tumor microenvironment, Inducible nitric oxide synthase (iNOS), Cyclophosphamide, L-n6-(1-iminoethyl)-lysine (L-NIL), Chemoradiotherapy, Radiotherapy, Head and neck squamous cell carcinoma, Head and neck cancer, Human papillomavirus (HPV)

* Correspondence: aurelie.hanoteau@gmail.com; Andrew.Sikora@bcm.edu

¹Department of Otolaryngology-Head and Neck surgery, Baylor College of Medicine, Houston, TX, USA

Full list of author information is available at the end of the article



Background

Head and neck squamous cell carcinoma (HNSCC) is the 6th most common cancer worldwide and has a poor prognosis at advanced stages of disease [1]. Human papillomavirus (HPV)-associated cancer of the oropharynx (throat) has become the fastest-increasing HNSCC subtype in the US and other developed countries, with the HPV16 viral type accounting for roughly 80% of HPV-positive HNSCC (HPV-HNSCC) [2]. Transformation of epithelial cancer cells by HPV16 depends on expression of the onco-viral proteins, E6 and E7 [3], which have also been shown to enhance intratumoral CD8⁺ T cell infiltration [4]. This enhanced immune response likely contributes to improved response and survival rates of HPV-HNSCC after chemoradiotherapy (CRT) compared to HPV-negative HNSCC [5] highlighting the potential role of tumor immune microenvironment as a determinant of CRT treatment response.

The standard-of-care CRT, consisting of tumor-directed radiotherapy and concurrent platinum-based chemotherapy (cisplatin or carboplatin) [6], is highly effective for the majority of primary HPV-HNSCC patients, but exhibits high failure rates in patients with locoregionally advanced, and recurrent or metastatic disease [7, 8]. Increasing evidence suggests that CRT simultaneously induces pro- and anti-tumoral immune responses [9]. CRT reportedly favors a number of anti-tumor mechanisms such as (i) improved antigen cross-presentation, (ii) increased Type I interferon release, and (iii) enhanced *major histocompatibility complex* (MHC) class I expression on tumor cells [10, 11]. However, it has also been linked to a variety of immunosuppressive effects including (i) the development of chemotherapy-resistant regulatory T cells (Tregs) [12], (ii) increased levels of circulating MDSCs (iii) the depletion and exhaustion of tumor-reactive T cells [13], and (iv) inhibition of T cell reactivity [14]. The multi-faceted immunomodulatory effects induced by CRT are limiting factors in its ability to stimulate effective immunological responses against solid tumors. Thus, immunomodulation of the tumor microenvironment is a promising approach to enhance the efficacy of CRT in solid tumors.

During cancer development, the tumor-mediated aberrant expression of inflammatory molecules contributes to the induction and intratumoral infiltration of immunosuppressive cells, such as MDSCs and Tregs. One such inflammatory mediator, inducible nitric oxide synthase (iNOS), is highly upregulated in numerous solid tumors [15, 16], and favors tumor growth through the enhanced induction and recruitment of MDSCs [17]. iNOS inhibition, such as with the iNOS-selective small molecule inhibitor L-n6-(1-iminoethyl)-lysine (L-NIL) [18] which has previously been tested in clinical trials for asthma and inflammatory disease [19], induces both immune-dependent and independent anti-tumor effects.

However, we have demonstrated that iNOS inhibition also increases Treg development and suppressive function [20]. To address this, we determined that cyclophosphamide (CTX) is an ideal complement to iNOS inhibition due to its ability to deplete Tregs [21]. Additionally, CTX enhances T cell activity and specificity by changing the T cell receptor (TcR) clonality [22–24]. We further demonstrated that the therapeutic combination of CTX with L-NIL decreases intratumoral MDSC and Treg levels and increases CD8⁺ T cell infiltration [20], leading to enhanced anti-tumor effects. This suggests that the combination of CTX/LNIL can positively re-condition the tumor immune microenvironment, with the potential to enhance the efficacy of other therapeutic regimens, such as CRT. We therefore hypothesized that adjuvant CTX/L-NIL could reverse the hostile tumor microenvironment, thereby enhancing the immunologic benefit of CRT.

To test this hypothesis, we used a syngeneic murine tumor model of HPV-HNSCC (mEER) featuring murine pharyngeal epithelial cells transformed with HPV16 E6 and E7 oncogenes and H-ras [25]. The mEER tumor model was chosen because its response to CRT has previously been shown to depend on an intact immune response [26] and it contains viral antigens (HPV16 E6/E7) suitable for monitoring antigen-specific T cell responses. Herein, we show that, while CTX/L-NIL or CRT alone induce modest tumor regression their combination significantly improved treatment efficacy, leading to an average of 21% complete tumor rejection in a CD8⁺ T cell-dependent manner. This enhanced response was attributed to significant improvement in the tumor immune microenvironment including (i) favorable alterations in the tumor myeloid compartment, (ii) an increase in the ratio of CD8⁺ T cells/ Tregs and (iii) increased infiltration of HPV16 E7-specific CD8⁺ T cells. These results suggest that modulation of the tumor immune microenvironment is an effective approach to improve treatment efficacy of conventional CRT in HPV-HNSCC and other solid tumors.

Methods

Mice

C57BL/6J male mice were purchased from The Jackson Laboratory and housed under specific pathogen-free conditions in standard temperature and lighting conditions with free access to food and water. Tumor inoculation was performed when mice reached 8–10 weeks of age. All experiments were performed with approval of the Institutional Animal Care and Use Committee (IACUC) at Baylor College of Medicine (BCM) and followed established protocols.

Tumor models

MEER tumor cell line expressing HPV16 E6, E7 and hRas was obtained from Dr. Chad Spanos at the Sanford

Research center/ University of South Dakota and maintained in E-media as previously described [26]. C57BL/6 J mice were injected subcutaneously (s.c.) with 10^6 mEER cells in the flank.

MOC2 cell line was a generous gift from Dr. Ravindera Uppaluri at Brigham and Women's Hospital/ Harvard Medical School and maintained as previously described [27]. C57BL/6 J mice were injected subcutaneously (s.c.) with 15×10^4 MOC2 cells in the flank.

Mice were monitored twice a week for tumor growth. Measurements were performed by using calipers and tumor area (mm^2) is expressed as $L \times W$, where L is Length and W is Width. Growth curve experiments were stopped once tumors reached 225 mm^2 .

In vivo treatment

All mice were randomized prior to treatment. Once tumors become established (average tumor size of 65 mm^2 or 19 mm^2 , day 17–18 or 8 after mEER and MOC2 inoculation, respectively) treatment was initiated over two weeks. The chemoradiotherapy treatment combined a fractionated tumor-directed radiation regimen (10 X 3Gy daily) (see Supplementary Material for further details) with weekly cisplatin ($83 \mu\text{g}/\text{mouse}$; Selleck Chemicals) intraperitoneal injections. The immunomodulatory treatment combined weekly intraperitoneal injections of cyclophosphamide ($2 \text{ mg}/\text{mouse}$; TCI Chemicals) and continuous oral administration of L-NIL (0.2%; Enzo Life Sciences) in the drinking water ad libitum.

For CD8 depletion experiments, all mice received the combinatory treatment and were injected with 1 mg depleting *InVivoMab* anti-mouse CD8 α (clone 53–6.7; BioXCell) or *InVivoMab* rat IgG2a isotype control (clone 2A3; BioXCell) 2 days prior the treatment, and further treated with weekly $250 \mu\text{g}$ antibodies for 3 consecutive weeks.

Human primary tumor Immunophenotyping

The 9 patients included in this study were part of a larger ($N=51$) published cohort of HPV⁺ OPSCC patients [28, 29]. All 9 patients included in this study received standard-of-care adjuvant (chemo) radiotherapy following surgical resection of their primary tumor. An overview of patient characteristics and treatments received is available in the prior publication [29]. Patients were involved after signing informed consent and studies were conducted in accordance with the Declaration of Helsinki and approved by the local medical ethical committee of the Leiden University Medical Center (LUMC) and in agreement with the Dutch law.

Following tumor resection, high-dimensional single cell mass cytometry (cyTOF) analysis and functional studies were performed to analyze immune cell population tumor infiltration and cytokine of the general tumor

infiltrating lymphocyte. The tumor microenvironment was reanalyzed for the relative low and strong presence of immune cell phenotypes and grouped according to the presence (immune response positive (IR+)) or absence (immune response negative- (IR-)) of HPV16-specific T cell tumor infiltration [28, 29].

Flow cytometry

To characterize tumor immune cell infiltration, mEER tumors were harvested, digested and stained using the method previously described [30]. Briefly, tumors were digested in RPMI 1640 (Sigma-Aldrich) containing DNase I ($20 \text{ U}/\text{ml}$; Sigma-Aldrich), Collagenase I ($1 \text{ mg}/\text{ml}$; EMD Millipore) and Collagenase IV ($250 \text{ U}/\text{ml}$; Worthington Biochemical Corporation) prior to mechanical disaggregation to form single cell suspensions. Following digestion, tumor infiltrating leukocytes were enriched using Lymphoprep™ (STEMCELL Technologies). Single cell suspensions were also prepared from tumor-draining inguinal lymph node and spleen with additional lysis of splenic red blood cells (RBC) using RBC lysis buffer (Invitrogen). Leukocytes were blocked with anti-mouse CD16/CD32 Fc block (BD Biosciences) and stained using one of various antibody panels (Additional file 1: Table S1 and S2). The viability of cells was determined using LIVE/DEAD™ Fixable Blue Dead Cell Stain Kit (Invitrogen). For intracellular staining, cells were fixed and permeabilized with Intracellular Fixation and Permeabilization Buffer Set (eBioscience) and stained using the appropriate antibody panel (Additional file 1: Table S1). Data were acquired on a LSRII and LSR Fortessa (BD Biosciences) flow cytometers, for myeloid and T cell panels respectively, and analyzed using FlowJo v10 software (FlowJo, LLC).

Quantitative multiplex immunofluorescence

Sectioning and Staining: After harvesting, tumors were immediately fixed overnight in 10% neutral-buffered formalin. Fixed tumors were embedded in paraffin and sections were cut at a thickness of $5 \mu\text{m}$. Full-section slides of tumor tissues were stained using Opal multiplex 6-plex kits, according to the manufacturer's protocol (PerkinElmer), for DAPI, Epcam (polyclonal; Abcam, 1:100 dilution), CD3 (clone SP7; Spring Biosciences; 1:100 dilution), CD8 (clone 4SM15; ThermoFisher; 1:500), CD4 (clone 4SM95; eBioscience, 1:50), Foxp3 (polyclonal; ThermoFisher, 1:500), and Granzyme B (polyclonal; Abcam, 1:200). Single color controls and an unstained slide were also included.

Multispectral imaging and analysis: Multispectral image capture was done at 20X magnification using Vectra (PerkinElmer, Hopkinton, MA). Images were analyzed using inForm software version 2.4.1 (PerkinElmer) as

previously described [31]. Further details are presented in the Supplementary Materials.

Gene expression analysis

Tumor samples were harvested and flash frozen in liquid nitrogen. Total RNA was extracted with the RNeasy Mini Kit (Qiagen) as per the manufacturer's instructions. Gene expression profiling was performed on 100 ng RNA using the nCounter® PanCancer Immune Profiling Panel (NanoString Technologies, Inc) containing 770 genes involved in cancer immune response. Further details are presented in the Additional file 1.

In vitro CD8⁺ T cell cytotoxicity assay

To observe whether changes in the tumor myeloid compartment after treatment influence intratumoral CD8⁺ T cell cytotoxicity, CD8⁺ T cells were purified from the spleen of naïve C57BL/6J mice with a magnetic bead-based CD8⁺ T cell negative selection kit (Miltenyi Biotec) and CD11b⁺/CD11c⁺ cells were isolated from mEER tumors undergoing treatment using a magnetic bead-based CD11c and CD11b positive selection kit (Miltenyi Biotec). 10⁵ CD8⁺ T cells were co-cultured with 3X10⁴ CD11b⁺/CD11c⁺ cells in enriched DMEM (20% FBS, 2 mM L-glutamine, 1% non-essential amino acid, 1 mM sodium pyruvate, 50 nM 2-mercaptoethanol, 1% penicillin/ streptomycin; as previously described [32]) including 10 ng/ml IL-2 (BioLegend), 2 µg/ml anti-CD3 (clone: 145-2C11; BioLegend) and 5 µg/ml anti-CD28 (clone: 37.51; BioLegend). After 4 days of co-culture, CD8⁺ T cells were collected and co-cultured with 3X10³ mEER tumor cells at a ratio of 4:1 (CD8⁺ T cell: tumor) in enriched DMEM including IL-2 (10 ng/ml). After 24 h, tumor cell apoptosis was observed via Cytation Cell Imaging Reader (Biotek) and quantified via flow cytometry using an Annexin V/Dead Cell Apoptosis kit (Invitrogen).

Statistical analysis

Data sets were tested for Gaussian distribution using the D'Agostino-Pearson normality test. For parametric data sets, statistical significance was determined by: unpaired t test for two-tailed data and ANOVA test followed by selected comparison by Tukey's multiple comparison tests with multiple comparison correction. For non-parametric data sets, statistical significance was determined by: Mann-Whitney test for two tailed data and Kruskal-Wallis test followed by selected comparison by Dunn's multiple comparison tests with multiple comparison correction. Survival was analyzed by the Kaplan– Meier method using Log-rank test. (**p* < 0.05; ***p* < 0.01; ****p* < 0.001; *****p* < 0.0001; ns, non-significant). Outliers from flow cytometry analysis were determined using ROUT (Q = 1%) method.

Results

Tumor immune microenvironment remains “cold” following CRT

The immunosuppressive effects of CRT and attempts to overcome them have been well documented [33, 34]; however, development of immunomodulatory strategies capable of reversing the balance of CRT immune effects towards activation remains a critical need. To address this, we developed an immunomodulatory strategy capable of rendering the tumor immune microenvironment susceptible to CRT through a “cold” to a “hot” immunologic transition (Fig. 1, Additional file 1: Figure S1). In this study, immunologically “cold” tumors are best characterized by high immunosuppressive cell infiltrate (i.e. MDSC, Tregs), low anti-tumor immune cell infiltrate (CD8⁺ T cells, M1 macrophages, dendritic cells (DCs)), and a lack of immune-favorable gene expression. Alternatively, immunologically “hot” tumors present with favorable effector/suppressor immune cell ratios and evidence of anti-tumor immune activation.

To better understand the immune impact of CRT on the tumor immune microenvironment, we developed a clinically relevant treatment schedule based on the standard-of-care CRT regimen for HPV-HNSCC. Briefly, fractionated tumor-directed radiation (3 Gy X 10 fractions of radiation) was combined with weekly cisplatin for a total of 2 weeks (Fig. 1a). mEER cells were inoculated subcutaneously in the flank of mice and treatment was initiated once the established tumor reached approximately 65 mm² in size. CRT treatment of tumors induced modest decreases in tumor growth (Fig. 1b) and improvement in survival (Fig. 1c). Tumor gene expression analysis indicates that the tumor microenvironment remains immunologically “cold” at the midpoint of treatment (one week; Fig. 1f). Multiple immunologic gene sets commonly associated with anti-tumor responses (i.e. T cell and dendritic cell (DC) function, interleukins (ILs), antigen processing, MHC, chemokines and receptors) showed low levels of expression similar to those of untreated tumors (Fig. 1f).

Immune-responsive HPV16⁺ HNSCC human tumors display a “hot” immune microenvironment and improved treatment response

Based on the murine gene expression analysis we next assessed, in a cohort of human HPV16⁺ oropharyngeal squamous cell carcinoma (OPSCC) patients, whether a favorable tumor immune microenvironment could influence standard-of-care treatment benefit (Fig. 1d). Briefly, the 9 patients included in this study received standard-of-care (chemo) radiotherapy following surgical resection of their primary tumor. Patients were grouped based on the presence (immune response positive (IR+)) or absence (immune response negative- (IR-)) of HPV16-specific T cell

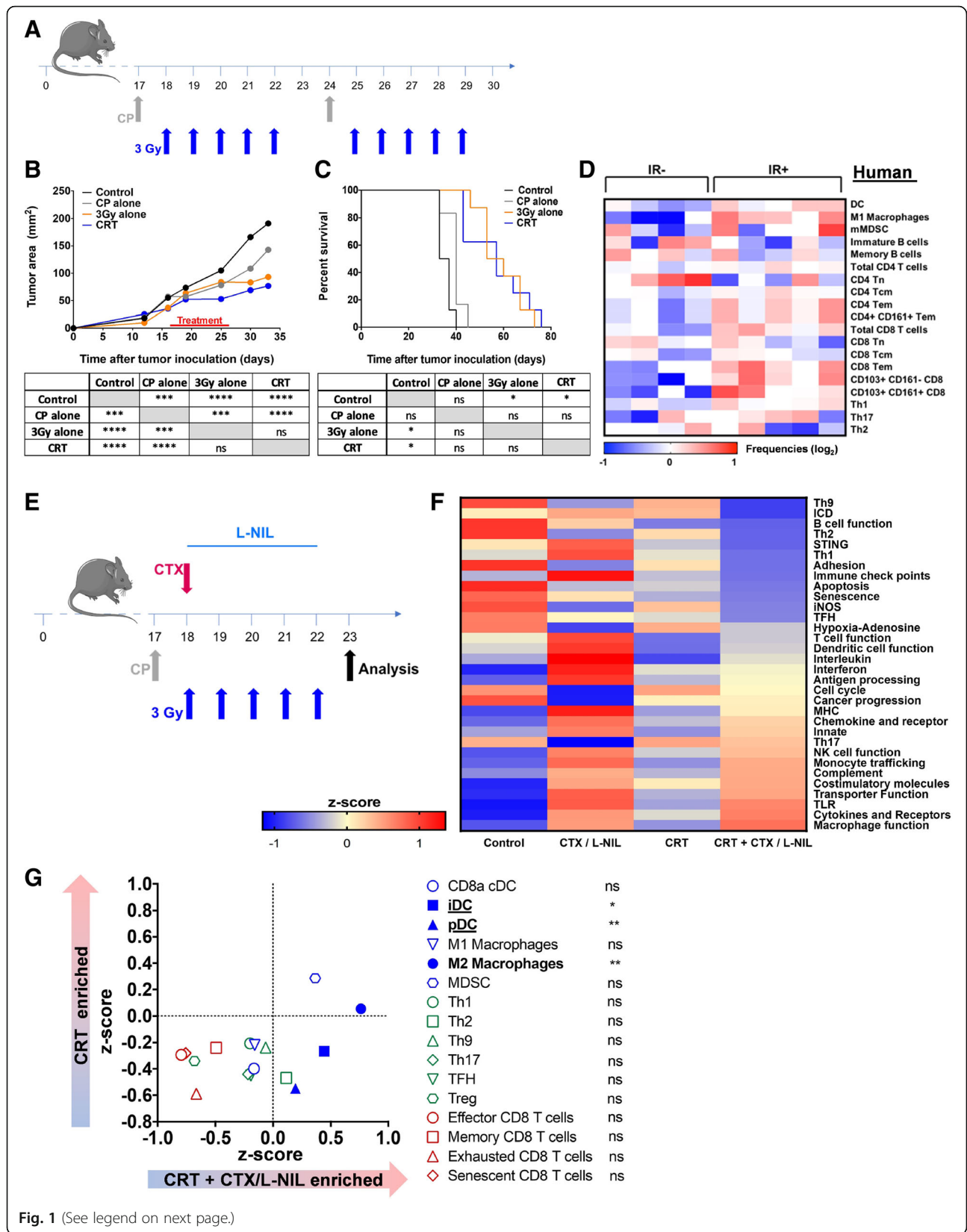


Fig. 1 (See legend on next page.)

(See figure on previous page.)

Fig. 1 CTX / L-NIL reverses the unfavorable immune microenvironment of CRT treated tumors. **a-c** Subcutaneous established mEER tumors (day 17–18 post tumor cell injection) were treated with tumor-directed radiation (5 X 3Gy) and/or weekly cisplatin (83 µg/mouse) i.p. injections, according to the schedule in **(a)**; mice were euthanized when tumors reached 225 mm². **b** Average tumor area (top) and statistical comparison of tumor sizes at time of first euthanasia (bottom; Tukey's multiple comparison test). **c** Survival curves (top) and statistical comparison between treatments (bottom; Log-rank test); **(b and c; N = 1** representative of 2; *n* = 6–8/group). **d** Heatmap depicting the relative abundance of various immune cell populations from CyTOF analysis in HPV16 immune reactive (IR+) and non-reactive (IR-) OPSCC human tumors based on the presence of HPV16-specific tumor infiltrating lymphocytes (TIL). Frequencies of DC (CD14⁺HLADR⁺CD11c⁺), M1 macrophages (CD163⁺CD14⁺HLA-DR⁺), monocytic MDCs (mMDSC; CD14⁺HLADR⁺), immature B cells (IgM⁺CD38⁺CD20⁺), memory B cells (IgM⁺CD38⁺CD20⁺), total CD4 and CD8⁺ T cells, naïve (Tn; CD45RA⁺CCR7⁺), central memory (Tcm; CD45RA⁺CCR7⁺) and effector memory (Tem; CD45RA⁺CCR7⁻) CD4⁺ and CD8⁺ T cells, CD4⁺CD161⁺ Tem, CD103⁺CD161⁻ and CD103⁺CD161⁺ CD8⁺ T cells. Th-denotation in indicates amount of IFN γ (Th1), IL-5 (Th2) and IL-17A (Th17) produced by the total TIL culture upon phytohemagglutinin stimulation. All data depicted as log-transformed values (base 2) relative to the median for each individual parameter and each column represents an individual patient (*n* = 9 total patients). **e-f** Established mEER tumors were treated with CRT and/or CTX/L-NIL immunomodulation (CTX at 2 mg/mouse i.p. and L-NIL at 0.2% in drinking water) and total tumor RNA was extracted and processed for gene expression analysis after 1 week of treatment, according to schedule in **(e)**. **f** Heatmap of differential immune gene-set pathway enrichment represented as z-scores between treatment groups (See Additional file 1: Table S3 for immune pathway gene list). **g** Gene-set based immune cell type enrichment comparing CRT and CRT + CTX/L-NIL represented as z-scores (left; See Additional file 1: Table S4 for immune cell type gene list) and statistical comparison for each immune cell type (right; unpaired t test); **(e and f; N = 1; n = 9/group)**. **p* < 0.05; ***p* < 0.01; ****p* < 0.001; *****p* < 0.0001; ns, not significant

tumor infiltration observed prior to treatment as previously described [28, 29]. In a prior study, IR+ OPSCC patients treated with surgery followed by adjuvant CRT were shown to have a 3-fold improvement in 5-year survival compared to IR- (ca. 90% vs 30%) [28, 29]. In our study, immune cell type analysis showed that the immune microenvironment of non-responsive (IR-) tumors was “cold” compared to that of immune-responsive (IR+) OPSCCs. IR+ tumors showed increased levels of several immune-stimulating myeloid subsets (i.e. dendritic cells and M1 macrophages) and effector lymphoid subsets (i.e. effector memory CD8⁺ T cells and Th1), thus linking quality of innate and adaptive intratumoral responses to treatment benefit (Fig. 1d). Together, these observations suggest that modulation of the tumor immune microenvironment to an immune responsive phenotype could increase the efficacy of standard-of-care CRT treatment.

CTX/LNIL immunomodulation reconditions the unfavorable tumor immune microenvironment

To activate the tumor immune microenvironment, we utilized an immunomodulatory treatment previously developed by our group [20] combining weekly CTX injections with continuous delivery of the iNOS inhibitor, L-NIL, in drinking water (Additional file 1: Figure S1A). To first characterize the immunomodulatory effects of the CTX/LNIL regimen in murine tumors, gene expression analysis was used to study the effects of each component of the treatment. Principal component analysis (PCA) revealed aggregate differences in gene expression and clustering based on treatment component (Additional file 1: Figure S1B; PC1 explained 54.13% and PC2 explained 14.25% of the observed variance). Immune gene-set analysis further revealed a “cold to hot” immunologic transition of the tumor following CTX and CTX/LNIL treatments (Additional file 1: Figure S1C).

This dataset and existing literature [23, 35] support the notion that CTX treatment induces favorable immunomodulatory effects. Nevertheless, its combination with L-NIL further enhances immune activation and favors a unique immunologic gene-set upregulation including STING, innate response, and Th1. Further immune cell type enrichment analysis revealed gene signatures consistent with increases in favorable myeloid and lymphoid subsets following CTX and CTX/LNIL treatment (Additional file 1: Figure S1D). Interestingly, CTX/LNIL promoted significant enrichment of effector CD8⁺ T cells and Th1 cells compared to CTX alone, consistent with the infiltrates found in immune responding HPV16⁺ OPSCC human tumors (Fig. 1d). Together, these observations showed that the combination of CTX and L-NIL functions as a potent immunomodulatory regimen capable of multifactorial enhancement of the intratumoral immune microenvironment.

Immune-suppressive effects of CRT are reversed by CTX/LNIL immunomodulation

Given the potent immunomodulatory effects induced by CTX/LNIL treatment, we hypothesized that this combination could improve the tumor immune microenvironment, rendering HPV-HNSCC tumors more responsive to CRT. Thus, we developed a combination treatment regimen in which mice bearing established mEER tumors were treated with concurrent CRT and CTX/L-NIL immunomodulation and we profiled the tumors for gene expression changes after the first week of treatment (Fig. 1e). PCA analysis revealed unique clustering of the combinatory CRT + CTX/L-NIL from that of CRT alone, but a similar clustering pattern is noted in comparison of CTX/LNIL and CRT + CTX/LNIL (Additional file 1: Figure S2A; PC1 explained 43.87% and PC2 explained 18.22% of the observed

variance), revealing that CTX/LNIL further modulates the CRT-induced tumor immune microenvironment. These data are further supported by immune gene-set analysis showing that numerous anti-tumor immune response pathways downregulated by CRT were upregulated by CRT + CTX/L-NIL, including MHC, toll-like receptor (TLR), complement system, antigen processing, DC and T cell functions (Fig. 1f; for individual sample heat map see Additional file 1: Figure S2B). Interestingly, several immunosuppressive pathways (i.e. iNOS, hypoxia-adenosine and immune check points) but also the immunogenic cell death (ICD) pathway that were upregulated by CRT strongly decreased in expression after the combinatory treatment. Additional immune cell type enrichment analyses highlighted a significant increase in several innate immune cell gene subsets following the combinatory CRT + CTX/L-NIL treatment; however, only inflammatory and plasmacytoid DCs were significantly upregulated compared to CRT alone (Fig. 1g). Overall these results show that, at the level of gene expression, CTX/L-NIL enhances favorable and suppresses unfavorable intratumoral immunologic effects of CRT.

CRT combined with CTX/L-NIL induces durable control of established tumors

To determine the therapeutic benefit of CRT and/or CTX/L-NIL immunomodulation, we assessed tumor growth and survival (Fig. 2). Briefly, mice bearing established mEER tumors were treated with CRT and/or CTX/L-NIL over a period of two weeks and were then continually monitored for long-term survival (Fig. 2a). While CRT and CTX/LNIL treatments alone each induced modest tumor growth delays compared to untreated mice, neither promoted complete tumor clearance. The combination of CRT + CTX/L-NIL significantly delayed tumor growth compared to singlet treatments and induced an average of 21% complete tumor clearance (12.5 to 30% depending on the experiment; Fig. 2b to d). To further validate these findings and determine if the treatment benefit was restricted to HPV-positive tumors, which bear viral antigens and typically have a better response to CRT, we next assessed the effects of combinatory treatments in an aggressive HPV-negative HNSCC cancer model, MOC2 [36] (Additional file 1: Figure S3). MOC2 cells were injected subcutaneously in the flank of mice and treatment was initiated once tumors became established (approximately 19 mm² in size; Additional file 1: Figure S3A). Combinatory treatment significantly delayed tumor growth compared to CRT and CTX/LNIL alone (Additional file 1: Figure S3 B and C) and increased overall survival by 23 days compared to conventional CRT (Additional file 1: Figure S3D). Collectively, this dataset shows that CTX/LNIL immunomodulation enhances the treatment benefit of conventional CRT regardless of

HPV-status, suggesting that this therapeutic approach may be applicable to treatment of a variety of solid tumors.

CTX/L-NIL favorably reprograms the myeloid tumor microenvironment in CRT treated tumors

We have previously shown that CTX/L-NIL inhibits the intratumoral infiltration of immunosuppressive MDSCs [20] and our prior gene expression analysis revealed numerous anti-tumor innate gene-sets and cell types enriched following CRT + CTX/LNIL treatment compared to CRT alone (Fig. 1f and g). Overall, these observations suggest that CTX/LNIL immunomodulation may favorably alter the myeloid tumor microenvironment. Thus, using flow cytometry, we assessed the impact of CTX/LNIL and/or CRT treatment on the tumor myeloid composition and function (Fig. 3). To eliminate immunologic bias due to tumor size, we chose to isolate tumors and observe the immune response at an intermediate treatment timepoint (after one week) when tumor sizes were comparable between all groups (similar to Fig. 1e). The analysis of myeloid cell subpopulations (among CD11b⁺/ CD11c⁺ cells) was performed using flow cytometry (for myeloid gating strategy see Additional file 1: Figure S4A, as previously described in [37]).

Due to the complexity of representing multiple immune subsets comprehensively, we utilized t stochastic neighborhood embedding (tSNE) to map high dimensional data onto two dimensional graphs [38]. tSNE analysis visually demonstrates strong myeloid subtype variation correlating to treatment (Fig. 3a) and quantification of these data shown as Z-scores in the radar plot highlights this effect (Fig. 3b). Among the subpopulations assessed, percentages of both inflammatory monocytes (characterized by the expression of CD11b⁺, MHCII^{low}, Ly6C⁺, CCR2⁺, CX3CR1⁺, iNOS⁺ (Additional file 1: Figure S4B)) and M1-like macrophages were increased following CTX/LNIL treatment. These two populations are further increased 2-fold and 1.6-fold, respectively, with CRT + CTX/LNIL compared to CRT alone (Fig. 3c and d). Furthermore, CRT + CTX/L-NIL significantly reduced the percentage of the immunosuppressive granulocytic MDSCs by 2-fold compared to CRT (Fig. 3e). Since both inflammatory monocytes and M1-like macrophages have been reported to support anti-tumor immune responses [39] and granulocytic MDSC are known to be highly immunosuppressive, this suggests that CRT + CTX/LNIL promotes the development of a beneficial myeloid tumor microenvironment.

Myeloid profiling was also performed in other lymphoid organs during treatment, in particular draining lymph nodes (dLNs) and spleen (Additional file 1: Figure S5). In the dLNs, CRT + CTX/L-NIL promoted a 2.8-fold decrease in granulocytic MDSCs compared to CRT

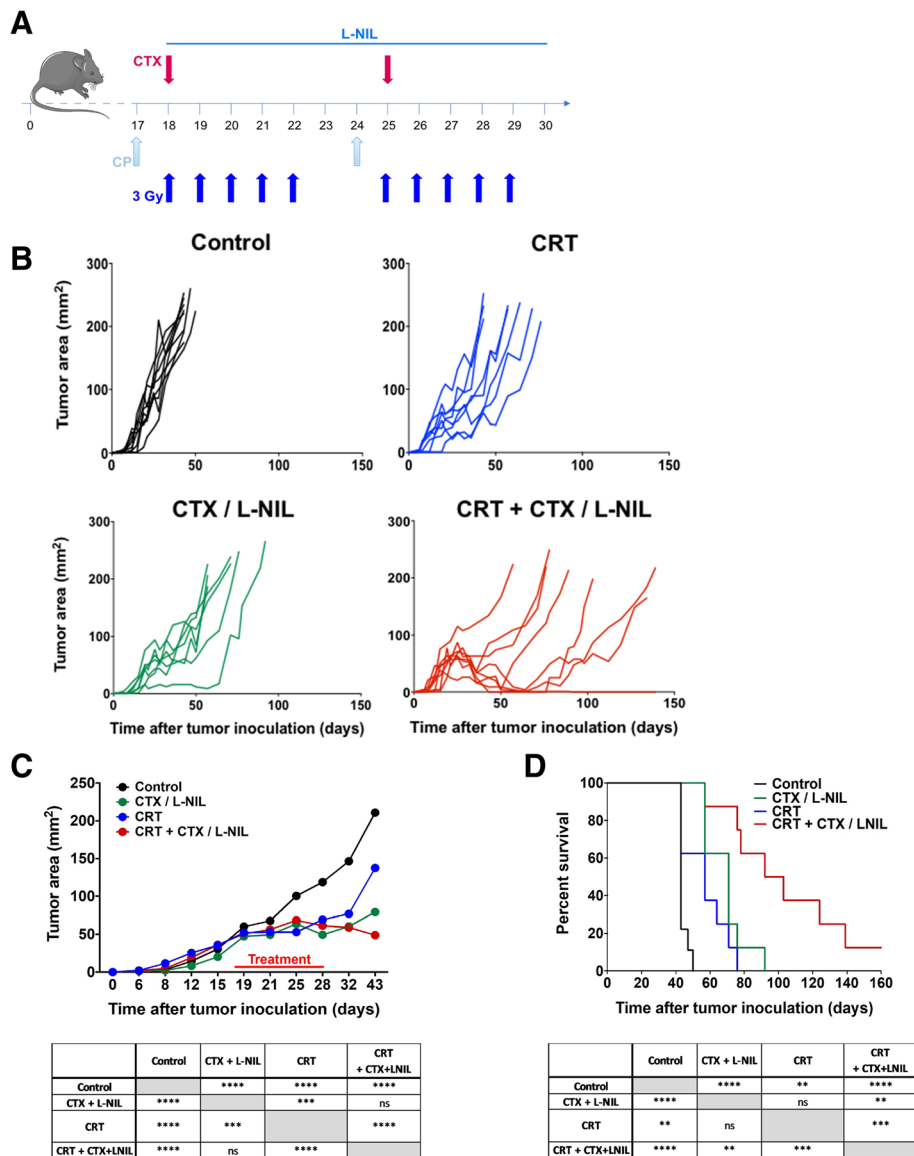


Fig. 2 CTX/L-NIL combines with CRT to induce durable control of established tumors. Mice bearing established mEER tumors were treated with CRT (10 X 3Gy tumor-directed radiation and 83 µg/mouse weekly cisplatin i.p.) and/or CTX/L-NIL immunomodulation (CTX at 2 mg/mouse i.p. and L-NIL at 0.2% in drinking water) according to the schedule in (a); mice were euthanized when tumors reached 225 mm². **b** Individual tumor growth curves shown by treatment group, with each mouse represented as a single line. **c** Average tumor area (top) and statistical comparison at time of first euthanasia (bottom; Tukey's multiple comparison test). **d** Survival curves (top) and statistical comparison between treatments (bottom; Log-rank test). (b-d; N = 1 representative of 2; n = 8-9/group). **p < 0.01; ***p < 0.001; ****p < 0.0001; ns, not significant

(Additional file 1: Figure S5 C), however, no other notable changes among myeloid subsets were observed in dLNs and spleen (Additional file 1: Figure S5 A-H). This suggests that the effects induced by the combinatory treatment are strongly localized to the tumor microenvironment. Overall, these observations demonstrate that CTX/L-NIL immunomodulation can be combined with CRT to favorably reprogram the tumor myeloid microenvironment, increasing cell subtypes known to benefit anti-tumor immune responses (inflammatory monocytes and M1-like macrophages) and

decreasing immunosuppressive cell subsets (granulocytic MDSCs).

Improved myeloid tumor microenvironment facilitates CD8⁺ T cell cytotoxic response

Since myeloid cells can both promote and suppress T cells according to their subtype and activation status [40], we sought to determine whether the favorable shift in the myeloid microenvironment induced by combinatory treatment influenced T cell anti-tumor cytotoxicity.

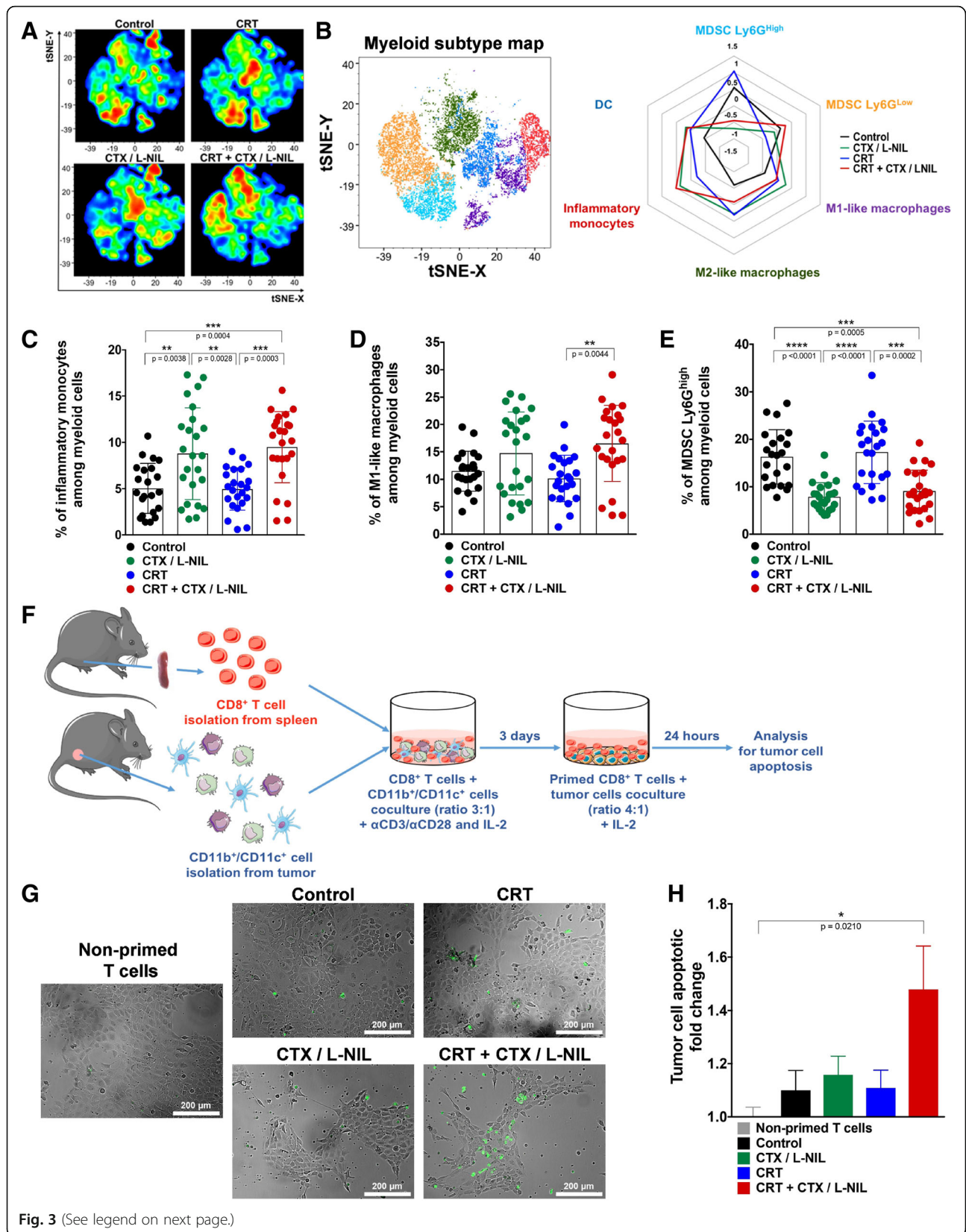


Fig. 3 (See legend on next page.)

(See figure on previous page.)

Fig. 3 CRT + CTX/L-NIL reprograms the myeloid tumor microenvironment. Established mEER tumors were treated with CRT and/or CTX/L-NIL and harvested after the first week of treatment, as shown in to Fig. 1e, and tumor myeloid cell infiltrate was analyzed using flow cytometry (**a-e**; see Additional file 1: Figure S4 for myeloid flow cytometry gating strategy) and ex vivo co-culture (**f-h**). **a** Myeloid-focused tSNE (among CD11b⁺/CD11c⁺ cells) from flow cytometry data for each treatment group. **b** Corresponding tSNE color-map (left) and radar plot (right) showing myeloid sub-type alterations between each treatment group as z-scores (myeloid sub-type color in radar plot corresponds with their color in tSNE map; $N = 1$ representative of 3; $n = 8-9$ /group). **c-e** Percentage of myeloid sub-types among total myeloid cell tumor infiltrate (CD11b⁺/CD11c⁺), including inflammatory monocytes (**c**), M1-like macrophages (**d**), and granulocytic MDSCs (**e**) ($N = 3$; $n = 23-25$ /group; Tukey's multiple comparison test for inflammatory monocytes and Dunn's multiple comparison test for M1-like macrophages and granulocytic MDSCs). **f** Experimental schematic used to test treatment-induced myeloid influence on CD8⁺ T cell cytotoxicity. Naïve splenic CD8⁺ T cells were stimulated with anti-CD3/CD28 antibodies and IL-2 in the absence or presence of myeloid cells (CD11b⁺ and CD11c⁺ cells) isolated from tumors that received different treatments for 3 days and then co-cultured with mEER cells in presence of IL-2. After 24 h, apoptotic tumor cells were detected by Annexin V / PI staining. **g** Representative images of mEER tumor cells stained for Annexin V (shown in green) following co-culture (scale bars show 200 μ m). **h** mEER tumor cell apoptotic fold change (Annexin V⁺ / PI⁻) normalized to non-primed T cells (T cells not co-cultured with myeloid cells) ($N = 4$; $n = 20-26$ /group; Dunn's multiple comparison test). All bar graphs show mean \pm SD and each dot represents an individual mouse. * $p < 0.05$; ** $p < 0.01$; *** $p < 0.001$; **** $p < 0.0001$

To assess this, we performed an ex vivo CD8⁺ T cell cytotoxic assay in which naïve splenic CD8⁺ T cells were stimulated (using anti-CD3, anti-CD28, and IL-2) in the presence of myeloid cells (CD11b⁺ and CD11c⁺ cells) isolated from treated tumors (as previously described in [32]). The myeloid-primed and stimulated CD8⁺ T cells were then co-cultured with mEER tumor cells and assessed for T cell induced cytotoxicity using Annexin-V/PI staining (Fig. 3f). Microscopic examination of Annexin V showed an increase in tumor cell apoptosis after CRT + CTX/L-NIL treatment compared to single therapies (Fig. 3g). Quantitative flow cytometry analysis revealed a significant improvement in the CD8⁺ T cell cytotoxicity, compared to non-primed stimulated CD8⁺ T cells, when influenced by the CRT + CTX/L-NIL intratumoral myeloid compartment (Fig. 3h). These data suggest that the favorable myeloid shift induced with the combination of CRT and CTX/LNIL lends to enhanced CD8⁺ T cell cytotoxicity.

CTX/LNIL improves the T cell tumor microenvironment in CRT treated tumors

Based on the above data and our previous report showing that CTX/LNIL immunomodulation promotes CD8⁺ T cell tumor infiltration [20], we assessed whether CTX/LNIL and/or CRT could favorably alter the intratumoral lymphoid compartment using multi-color immunofluorescence and flow cytometry (Figs. 4 and 5). After one week of treatment (similar to Fig. 1e) we profiled tumors by multiplex immunofluorescence [31]. We observed an increase in CD8⁺ T cell tumor infiltration and a higher level of cytoplasmic Granzyme B after CTX/L-NIL and combinatory treatment (Fig. 4a). Image quantification of T cell subsets further revealed that CTX/LNIL immunomodulation promoted a CD8⁺ T cell dominated tumor and a drastic depletion of Tregs, and this effect was maintained when combined with CRT (Fig. 4b). Additionally, we observed that CTX/LNIL improved CD8⁺ T cell activation compared to CRT, as evidenced by the

expression of cytoplasmic Granzyme B. When combined, although non-significantly, CRT + CTX/L-NIL induces a 4-fold increase in the intratumoral density of CD8⁺ T cells expressing Granzyme B compared to CRT alone (Fig. 4c).

To further characterize the influence of combinatory treatment on changes within the T cell tumor microenvironment, we performed flow cytometry (for lymphocyte gating strategy see Additional file 1: Figure S6A). tSNE analysis revealed qualitative shifts of intratumoral T cell subsets correlating to treatment (Fig. 5a). Further quantification revealed a 1.8-fold increase in the percentage of CD8⁺ T cells and a 3.4-fold decrease in Tregs after the combinatory CRT + CTX/LNIL treatment compared to CRT alone (Fig. 5b). These changes resulted in a 31.8-fold increase in the CD8⁺ T cell/Treg ratio after CRT + CTX/L-NIL compared to CRT alone (Fig. 5c). Further T cell subset analysis in other lymphoid organs demonstrated that the combinatory CRT + CTX/L-NIL treatment also reduced the percentage of Tregs in the dLNs (Additional file 1: Figure S7C) but not in the spleen (Additional file 1: Figure S7G) compared to CRT alone. The percentage of CD8⁺ and CD4⁺ T cells in dLNs (Additional file 1: Figure S7A and B) and spleen (Additional file 1: Figure S7E and F) were unchanged and thus the ratio of CD8⁺ T cells / Tregs was only significantly increased in dLNs but not in the spleen after CRT + CTX/L-NIL therapy compared to CRT alone (Additional file 1: Figure S7 D and H). Overall these data suggest that the combination of CRT and CTX/LNIL strongly and specifically activates the intratumoral T cell microenvironment.

CRT + CTX/L-NIL changes the phenotype of tumor-infiltrating CD8⁺ T cells

To further understand the consequences of the improved CD8⁺ T cell infiltration induced by the combinatory treatment, we next analyzed the tumor-infiltrating CD8⁺ T cells for various functional markers. We first tested

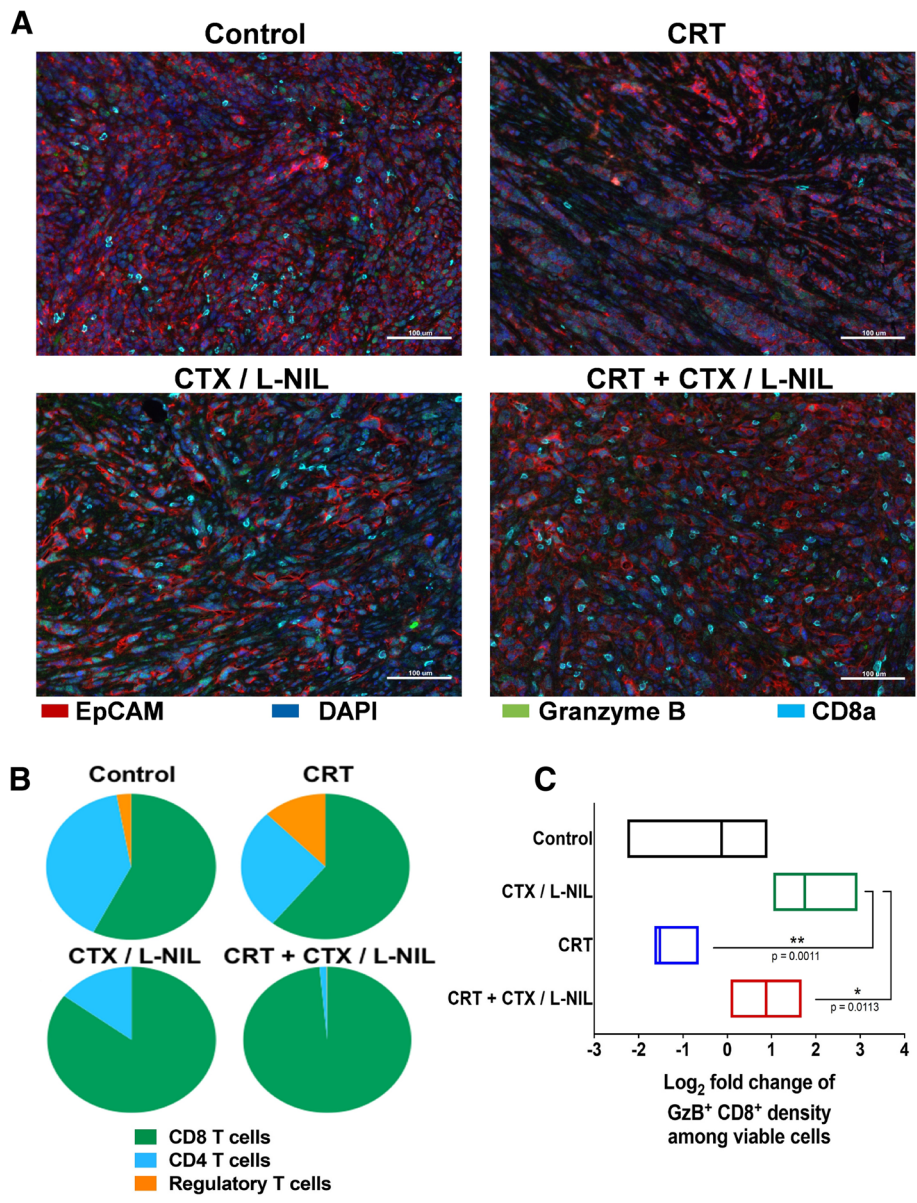
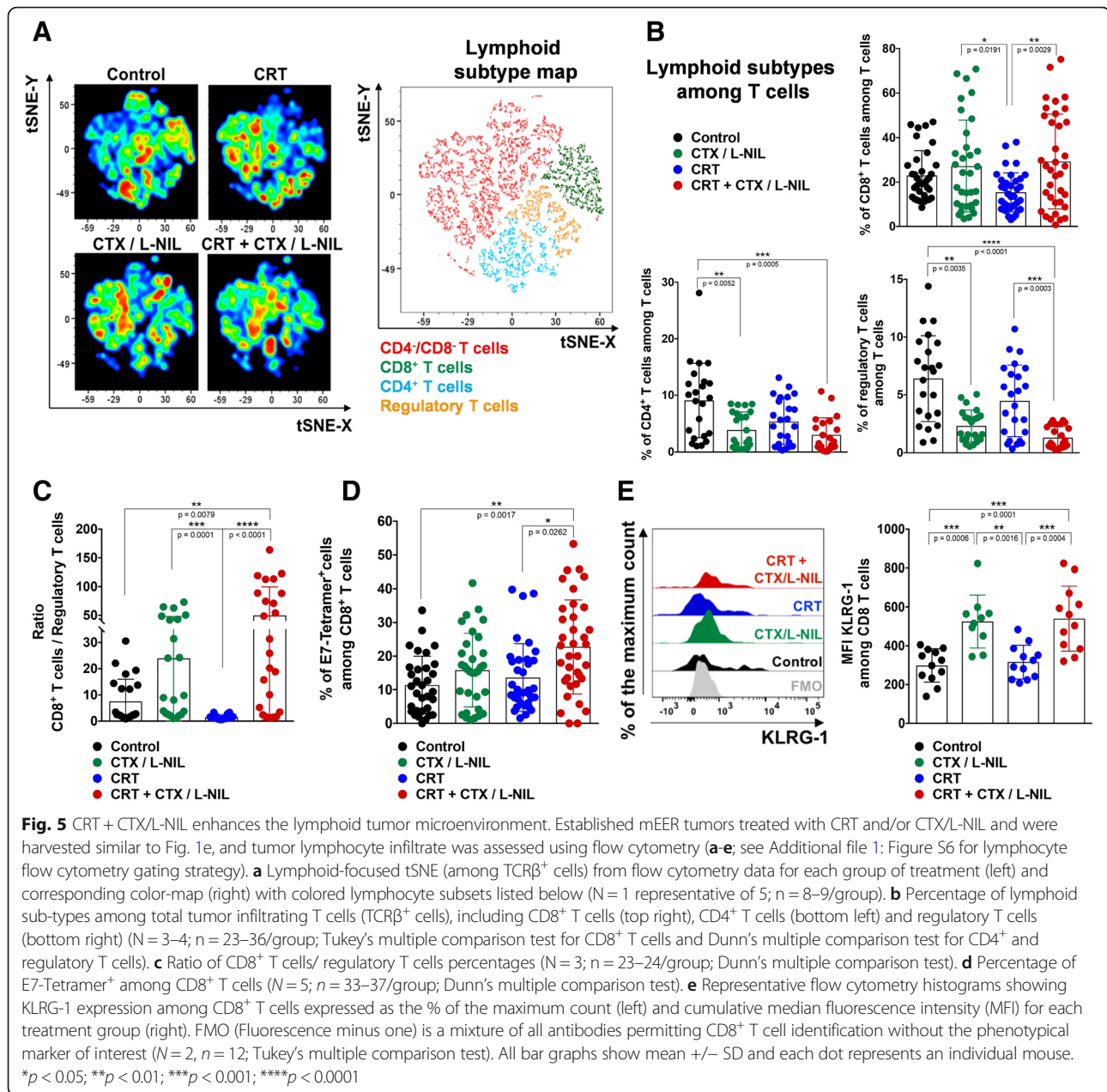


Fig. 4 CRT + CTX/L-NIL promotes intratumoral CD8⁺ T cell infiltration and activation. Established mEER tumors were treated with CRT and/or CTX/L-NIL and harvested after the first week of treatment, as shown in Fig. 1e, and tumor lymphocyte infiltrate was analyzed using quantitative multiplex immunofluorescence (qmIF; **a-c**). **a** Representative multiplex images of mEER tumors showing DAPI (nuclei, dark blue), EpCAM (tumor, red), CD8a (CD8⁺ T cells, cyan), and Granzyme B (T cell cytotoxic marker, green). **b** Pie-charts showing T cell subset fractions among total T cells for each treatment (fraction averaged across 5 images per tumor and $n = 3$ /group). **c** Log₂ fold change of Granzyme B (GzB)⁺ CD8⁺ cells normalized to control group ($N = 1$; $n = 3$ /group; Tukey's multiple comparison test). Bar graphs show mean \pm SD. * $p < 0.05$; ** $p < 0.01$

whether CRT + CTX/L-NIL could improve CD8⁺ T cell tumor specificity by evaluating E7-specific tetramers binding by flow cytometry (Additional file 1: Figure S6B). This revealed that the proportion of intratumoral CD8⁺ T cells specific for the E7 antigen expressed by mEER tumor cells was significantly increased following CRT + CTX/L-NIL treatment (more than 22.7% of CD8⁺ T cells on average) (Fig. 5d). Based on a consensus nomenclature defined for murine and human CD8⁺ T cell phenotypes [41], we

monitored the expression of several markers associated with T cell effector, memory, and exhaustion functions using flow cytometry (Fig. 5e and Additional file 1: Figure S8). CRT + CTX/L-NIL promoted a significant increase in the expression of killer cell lectin-like receptor G1 (KLRG1), a marker commonly associated with effector CD8⁺ T cell subsets [42]. However, perforin expression on CD8⁺ T cells was significantly decreased after CRT + CTX/L-NIL treatment compared to CRT alone, suggesting

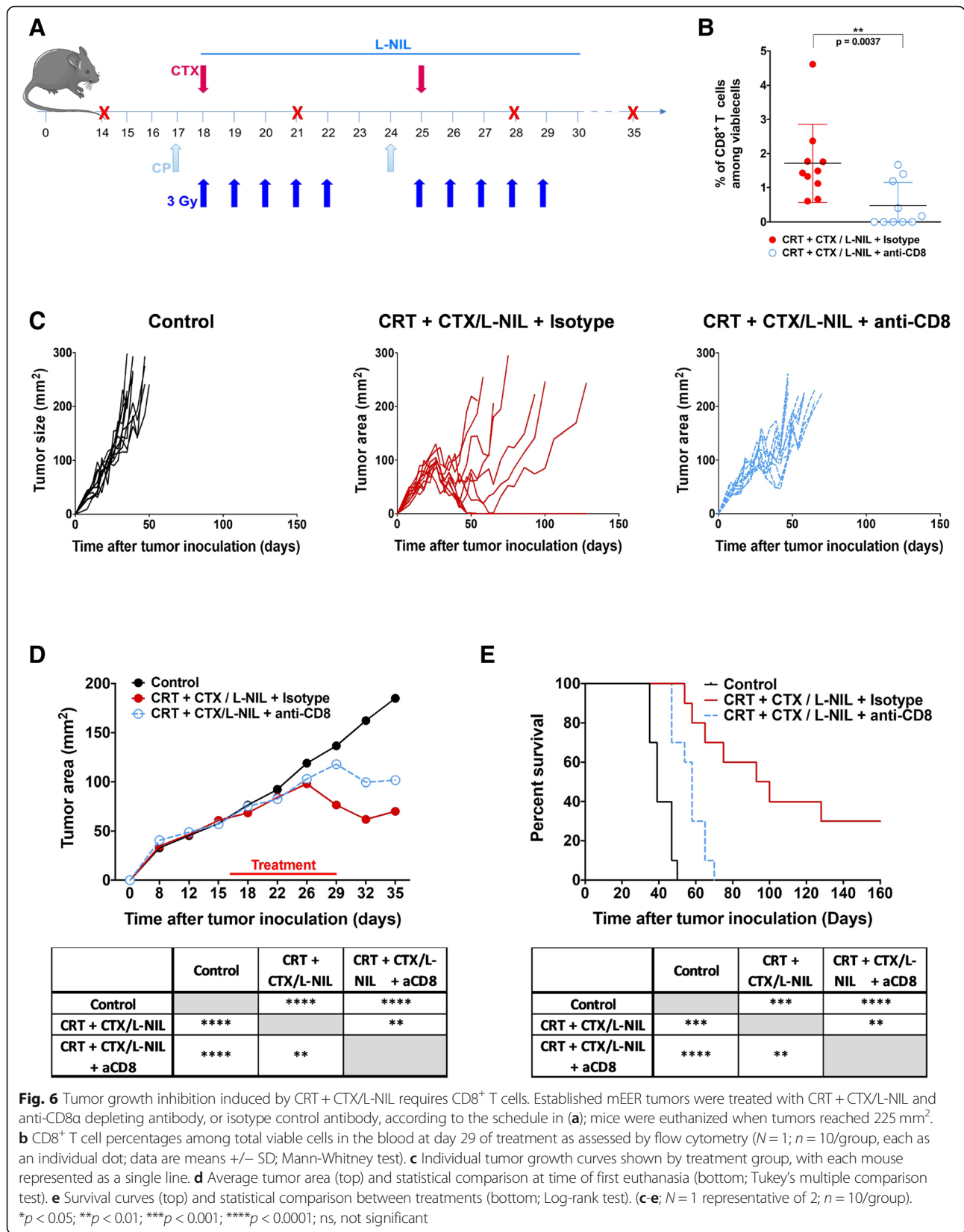


that CD8⁺ T cells had entered a later killing phase [43]. Collectively, these observations show that the tumor infiltrating CD8⁺ T cells promoted by the combinatory CRT + CTX/LNIL treatment exhibit improved specificity and effector phenotypes compared to CRT alone.

Tumor growth inhibition induced by CRT + CTX/LNIL is dependent on CD8⁺ T cells

Since our data show that CTX/L-NIL immunomodulation enhances susceptibility of immune-refractory tumors to CRT by changing the myeloid compartment, leading to enhancements in CD8⁺ T cell specificity and function, we examined whether improved tumor

regression and survival was dependent on CD8⁺ T cells (Fig. 6). To accomplish this, depleting anti-mouse CD8 antibodies were injected two days before treatment and then weekly over the course of CRT + CTX/LNIL treatment (Fig. 6a). Flow cytometry analysis validated the depletion of CD8⁺ T cells observed in the blood (Fig. 6b). In the absence of CD8⁺ T cells, the combinatory treatment induced a small tumor growth delay, compared to control tumors (Fig. 6c and d). The stall in tumor growth observed in the absence of CD8⁺ T cells is likely a combination of direct tumor cell killing by the chemotherapeutic and radiation components of the combination treatment and non-CD8-dependent cytotoxic



mechanisms (e.g. Natural Killer-mediated killing). Nevertheless, long term survival benefits are entirely lost in the absence of CD8⁺ T cells (Fig. 6e). These results confirm that CD8⁺ T cells are critical component of the therapeutic benefit induced by the combinatory CRT + CTX/LNIL treatment.

Discussion

Enhancing the efficacy of standard-of-care therapies, such as CRT, is a critical goal in the field of oncology. In HPV-associated HNSCC, treatment response has been correlated with tumor immune cell infiltration [5]. Additionally, CRT induces immunosuppressive effects which potentially limit its effectiveness [12, 13]. Thus, we hypothesized that therapeutic outcome of CRT could be improved through favorable modulation of the tumor immune microenvironment.

The multi-faceted immunosuppressive tumor microenvironment contains numerous potential therapeutic targets whose modulation could render the tumor microenvironment more immunologically favorable. Indeed, HNSCC tumors express various immunosuppressive cytokines such as *transforming growth factor beta* (TGF- β), IL-6 or IL-10 [44, 45] and enzymes which deprive the tumor microenvironment of essential nutrients for T cell function, such as indoleamine 2,3-dioxygenase (IDO)-mediated degradation of the amino acid tryptophan [46]. Several IDO inhibitors are currently in phase I/II clinical trials [47] and may constitute an effective immunomodulatory therapy to combine with CRT. Additionally, MDSCs were found to be present in high numbers in HNSCC tumors [48] and their enzymes, arginase-1 and iNOS, are known to drive immunosuppression partially by inactivating effector T cells [49, 50]. Small molecule inhibitors have been developed to target arginase-1 and iNOS, including nor-NOHA and L-NIL, respectively [51]. iNOS, in particular, has been shown to be overexpressed in many different solid tumors and implicated in both immunosuppressive responses and resistance to chemotherapy and radiotherapy [52, 53], which support the rationale for combining an iNOS inhibitor with standard-of-care CRT. We have previously shown that while iNOS inhibition using L-NIL can inhibit MDSC recruitment to the tumor, this compound also drives a compensatory increase in Treg infiltration. This is addressed through a combination immunomodulatory approach combining L-NIL with CTX, which promotes significant antitumor immune effects by depleting intratumoral MDSCs and Tregs, respectively [20]. Herein, our ultimate goal was to determine if CTX/L-NIL immunomodulation could reverse CRT-induced immunosuppressive effects and

enhance antitumor effector responses, thus maximizing its treatment efficacy.

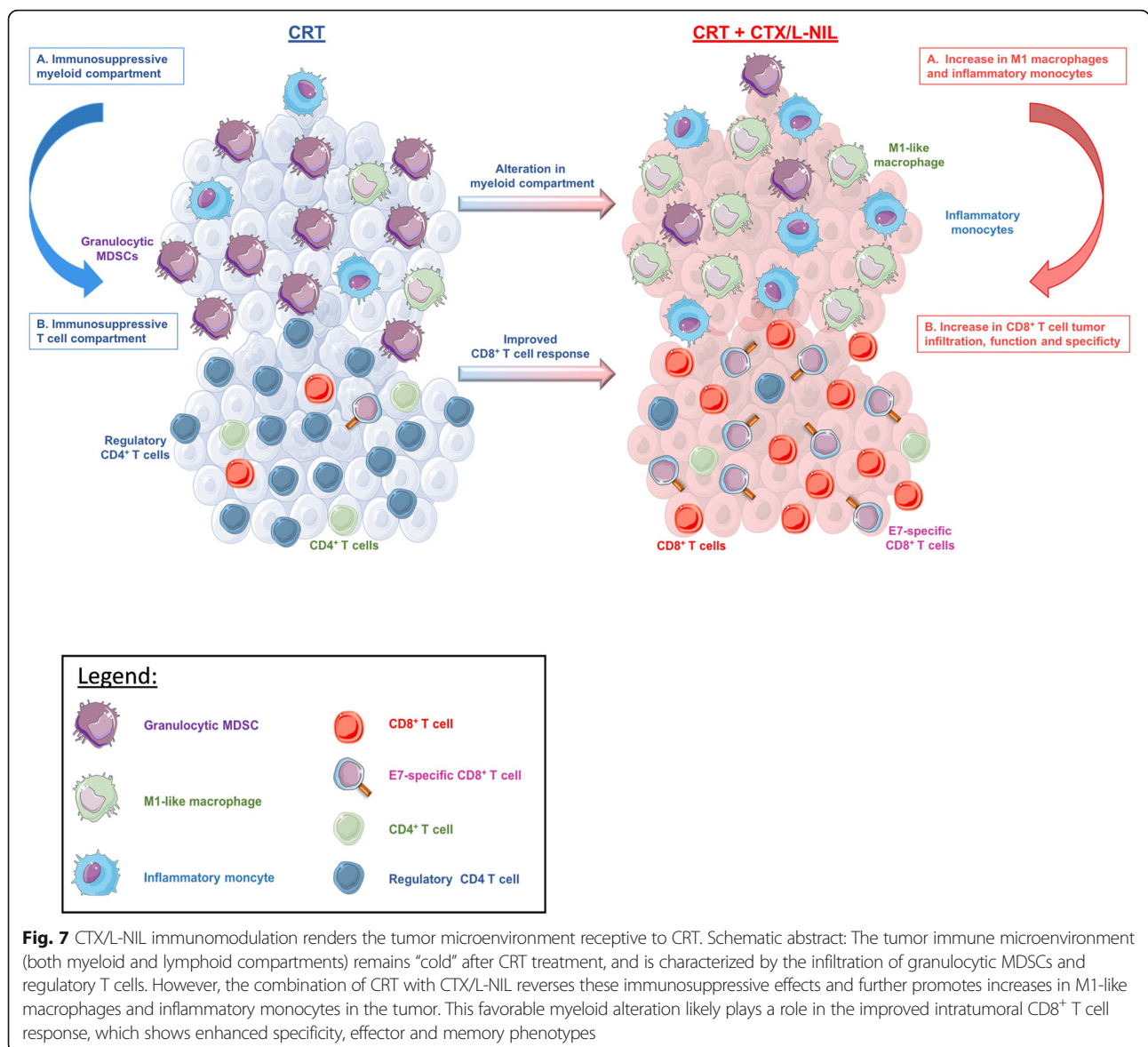
Toward this end, we developed a clinically relevant treatment model based on standard-of-care CRT administered to patients with HPV-HNSCC. In this model, we treated the syngeneic HPV-HNSCC mEER tumor line with fractionated (10 fractions of 3 Gy) tumor-directed radiation regimen and weekly cisplatin administration. This regimen is particularly important because different radiation schedules can induce drastically distinct immunologic responses and may even suppress immunity [14, 54]. Much of the preclinical literature studying CRT effects uses “hypo-fractionated” (small number of large doses) RT treatment schedules and shows a delay in tumor growth as well as an increased infiltration of innate and adaptive cells, such as DCs and CD8⁺ T cells in the tumor [55]. However, the infiltration of anti-tumor immune cells following hypo-fractionated radiation has also been shown to be temporally restricted and to occur primarily between 5 to 10 days after the first irradiation [55, 56]. We have also assessed the tumor immune response at various time points following our more conventionally fractionated regimen of CRT and observed that the tumor infiltration of DCs, CD8⁺ and CD4⁺ T cells reached a maximum after one week of treatment (data not shown). Our observation showed that fractionated radiation presents a timely restricted immune response similar to hypo-fractionated regimens, and the date we selected for analyzing the tumor microenvironment was during this peak window of immune cell infiltration. In addition to the clinical relevance of our selected treatment schedule, we also chose to assess the effects of therapeutic approaches in large, established tumors. This more accurately represents the clinical scenario, in which patients often present with advanced tumors which already have well-established immunosuppressive microenvironments. Thus, our data should provide a translationally-relevant understanding of the immunologic consequences of CRT as well as actionable therapeutic strategies for overcoming the immunological barriers.

Herein, we showed that CTX/L-NIL immunomodulation combined with CRT promoted significant enhancement of treatment efficacy, with 21% complete tumor rejection in a CD8-dependent manner. In tumors of mice receiving the combinatory treatment, we observed significant changes in the myeloid immune microenvironment, including an increase in various myeloid populations known to promote anti-tumor effects (i.e. inflammatory monocytes and M1-like macrophages) and a decrease in immunosuppressive granulocytic MDSCs. This modification in the myeloid microenvironment likely contributes to an improved T cell compartment within the tumor, including an increase in the ratio

CD8⁺ T cells/regulatory T cells and in the percentage of E7-specific CD8⁺ T cells compared to CRT alone. Gene expression analysis further corroborated these effects as it showed that CRT + CTX/L-NIL upregulated gene sets related to MHC, antigen processing, dendritic cell function, and induced a “hot” (activated) intratumoral immunologic state. Moreover, the analysis of tumor gene expression showed an increase in immunologic cell death (ICD) pathway compared to control group for each of singlet therapies (CRT or CTX/L-NIL), suggesting that these treatments favor ICD. Surprisingly, the ICD pathway appears to be decreased following the combination of CRT + CTX/L-NIL compared to singlet treatments, suggesting that induction of immunogenic cell death is not the major mechanism contributing to the efficacy of the combinatory treatment. Overall, our

results demonstrated that CTX/LNIL immunomodulation can greatly improve the treatment effects of CRT by heating up the tumor immune microenvironment (Fig. 7), towards a similar constitution that in the clinic has been associated with a favorable response to (chemo) radiotherapy (Fig. 1d and [28]).

While CD8⁺ T cell phenotype profiling showed an increase in markers of T cell memory, tumor rechallenge experiments revealed a lack of functional immunologic memory response (data not shown). This constitutes a limitation of our results and mandates further investigation to understand and address this limitation in long-term memory recall response. A number of recent studies suggest that radiation fractionation schedules may have significant treatment implications on the anti-tumor functionality of the immune system. Previous



work has shown that hypofractionated radiation schedules can increase the frequency of circulating T cells, and promote higher numbers of CD8⁺ T cells [57, 58]. Thus, future work will compare the immunologic consequences, especially those pertaining to immunologic memory, of different radiation fractionation schedules. Our work also suggests that immune microenvironment modulation could be utilized to improve treatment results of other immunotherapeutic approaches (i.e. immune checkpoint inhibitors, chimeric antigen receptor T cells, cancer vaccination strategies). This could potentially improve the memory response induced by our combination treatment, since immune checkpoint blockade with anti-CTLA-4 has been shown to enhance the generation of memory T cells in mice [59]. It is also likely that additional strategies to improve the number of HPV-E6/E7 specific CD8⁺ T cells, such as vaccination with long peptides against these antigens, could also improve the overall treatment benefit of this regimen [60].

In an effort to enhance the translatability of this work, we utilized a repurposing approach using two clinically-relevant drugs to overcome the negative effects of the tumor immune microenvironment. This combination included CTX, a widely utilized chemotherapeutic agent which is commonly used as an immunomodulator; and L-NIL, which has been tested in clinical trials for asthma and inflammatory diseases [19]. Despite the translational potential of this study, a few key issues remain to be addressed before clinical investigation of the CTX/LNIL immunomodulatory regimen. The first relates to the injection timing and the dose of CTX used, as this can have major influences on treatment response. Contrary to high dose CTX, which is lymphodepleting and cytotoxic, low dose of CTX is immune dependent, increases the anti-tumor immune response and favors T cell tumor infiltration [61]. In terms of treatment schedule, metronomic dosing has been previously tested in the clinic and was found to selectively deplete Tregs and improve overall T cell function and specificity [62, 63]. However, another study demonstrated optimal immunomodulating effects with a single injection of CTX slightly above the ablative dose [64]. Thus, a CTX dose titration and schedule-finding study would likely be necessary to establish the optimal immunomodulatory response. The second key issue relates to the iNOS inhibitor utilized in this study, L-NIL, which, despite prior testing in clinical trials for benign diseases, requires additional clinical assessment before it could be used for treatment of cancer patients. However, the efficacy of other commonly used drugs with iNOS inhibiting activity, such as doxycycline or phosphodiesterase 5 inhibitors (sildenafil and tadalafil), could be investigated in parallel to facilitate rapid translation to clinic trials [65–67].

Conclusion

In conclusion, our study demonstrates that immunomodulation of the tumor microenvironment can render refractory tumors susceptible to CRT. The clinical relevance of the models studied and the combination of standard-of-care CRT with repurposed immunomodulatory drugs has the potential to accelerate clinical translation of this approach.

Additional file

Additional file 1: Figure S1. The combination of CTX / L-NIL reverses the cold tumor microenvironment. **Figure S2.** CTX / L-NIL activates the immune microenvironment of CRT treated tumors. **Figure S3.** CTX/L-NIL improves CRT treatment effects in established HPV-negative tumors. **Figure S4.** Gating strategy for myeloid sub-types and inflammatory monocyte phenotyping. **Figure S5.** Systemic myeloid effects induced by CRT+CTX/L-NIL. **Figure S6.** Gating strategy for lymphocyte sub-types. **Figure S7.** Systemic lymphoid effects induced by CRT+CTX/L-NIL. **Figure S8.** CD8⁺ T cell phenotype in tumors. **Table S1.** Flow cytometry antibodies used for myeloid subset analysis. **Table S2.** Flow cytometry antibodies used for lymphocyte and CD8⁺ T cell subset analysis. **Table S3.** Immune pathway signature gene list used in gene expression analysis. **Table S4.** Immune cell type signature gene list used in gene expression analysis [68–70]. (ZIP 12061 kb)

Abbreviations

CRT: Chemoradiotherapy; CTX: Cyclophosphamide; DC: Dendritic cell; KLRG1: Killer cell lectin-like receptor; HNSCC: Head and neck squamous cell carcinoma; HPV: Human papillomavirus; ICD: Immunogenic cell death; IDO: Indoleamine 2,3- dioxygenase; IL: Interleukins; iNOS: Inducible nitric oxide synthase; IR-: Immune response negative; IR+: Immune response positive; L-NIL: L-n6-(1-iminoethyl)-lysine; MDSC: Myeloid-derived suppressor cell; MHC: Major histocompatibility complex; OPSCC: Oropharyngeal squamous cell carcinoma; PCA: Principal component analysis; s.c.: Subcutaneously; TGF-β: Transforming growth factor beta; TLR: Toll-like receptor; Treg: Regulatory T cell; tSNE: t Stochastic neighborhood embedding

Acknowledgments

The authors thank Dr. Yohannes Ghebre and Dr. Gretchen Diehl for their constructive feedback, and Dr. Ravindra Uppaluri for providing MOC2 tumor cell line. We further acknowledge the following core facilities: Cytometry and Cell Sorting Core facility at Baylor College of Medicine with funding from NIH (P30 A1036211, P30 CA125123, and S10 RR024 574) and the expert assistance of Joel M. Sederstrom, Genomic and RNA Profiling Core Facility at Baylor College of Medicine with funding from P30 Digestive Disease Center Support Grant (NIIDK-DK56338) and P30 Cancer Center Support Grant (NCI-CA125123) and the expert assistance of Mylinh Bernardi, Pathology and Histology core at Baylor College of Medicine, Flow Cytometry and Cellular Imaging Core Facility (FCCICF) at MD Anderson partially funded by NCI Cancer Center Support Grant P30CA16672 and the expert assistance of Jared K. Burks, Ph.D. We acknowledge Columbia University Irving Medical Center's Human Immune Monitoring Core (HIMC) for quantitative multiplex immunofluorescence and Vectra imaging platform.

Funding

J.M.N acknowledges financial support from the National Institute of General Medical Sciences T32 predoctoral training grant (T32GM088129) and the National Institute of Dental & Craniofacial Research F31 NRSA training grant (F31DE026682) both of the National Institutes of Health. This content is solely the responsibility of the authors and does not necessarily represent the official views of the National Institutes of Health. S.H.v.d.B. and S.J.S. acknowledge financial support from the Dutch Cancer Society 2014–6696. R.D.G. acknowledges support from Swim Across America. R. K. acknowledges financial support from the German Cancer Aid. B.Z. and C.H. were supported by grant CPRIT RR160027 from the Cancer Prevention and Research Institutes of Texas and by funding from the McNair Medical Institute at The Robert

and Janice McNair Foundation. JAVG and DL are supported by Kom op tegen Kanker (Stand Up against Cancer) and FWO (Science Foundation Flanders). JAVG is also supported by Foundation against Cancer. A.G.S. acknowledges support from the Caroline Weiss Law Endowment for Academic Excellence; the Owens Foundation; and grants from the Cancer Research Institute (Team Strategy Grant), and the National Institutes of Health (NCI/NIDCR 1U01DE028233–01).

Availability of data and materials

The majority of data obtained and materials used are presented in this publication or in supplementary material. Additional data or materials will be provided upon reasonable request and signing of a material transfer agreement.

Authors' contributions

AH, JMN, RK, and AGS designed the study, AH, JMN, H-CL, AG, FP, and PJ performed the immunological experiments, WCS provided mEER tumor cell line, DL and JAVG contributed myeloid expertise, CH, AH, JMN and BZ conducted gene expression analysis, RDG, YMS, JMN and TDH contributed to the multiplex analyses, SHvdB and SJS analyzed and provided human data analysis. AH conducted the statistical analysis, AH and JMN analyzed data and AH, JMN, and AGS interpreted the data. AH wrote the manuscript and JMN, AGS, DL and JAVG and CJM contributed to the manuscript corrections. All authors approved the final manuscript.

Ethics approval and consent to participate

All mice were housed and treated in accordance with Institutional Animal Care and Use Committee guidelines at Baylor College of Medicine. Patients were involved after signing informed consent and studies were conducted in accordance with the Declaration of Helsinki and approved by the local medical ethical committee of the Leiden University Medical Center (LUMC) and in agreement with the Dutch law.

Consent for publication

Not applicable.

Competing interests

R.D.G. has received travel support from PerkinElmer. A.G.S. receives support in the form of investigational drug from Advaxis for an investigator-initiated clinical trial.

Publisher's Note

Springer Nature remains neutral with regard to jurisdictional claims in published maps and institutional affiliations.

Author details

¹Department of Otolaryngology-Head and Neck surgery, Baylor College of Medicine, Houston, TX, USA. ²Interdepartmental Program in Translational Biology and Molecular Medicine, Baylor College of Medicine, Houston, TX, USA. ³Pathology of the University Hospital Schleswig-Holstein, Campus Luebeck and Research Center Borstel, Leibniz Lung Center, Lubeck and Borstel, Germany. ⁴Department of Molecular and Human Genetics, Baylor College of Medicine, Houston, TX, USA. ⁵Lester & Sue Smith Breast Center, Baylor College of Medicine, Houston, TX, USA. ⁶Department of Pediatrics, Division of Pediatric Hematology/Oncology, Columbia University Irving Medical Center/New York Presbyterian, New York, USA. ⁷Department of Medicine, Division of Hematology/Oncology, Columbia University Irving Medical Center/New York Presbyterian, New York, USA. ⁸Department of Medical Oncology, Leiden University Medical Center, Leiden, The Netherlands. ⁹Laboratory of Cellular and Molecular Immunology, Vrije Universiteit Brussel (VUB), Brussels, Belgium. ¹⁰Laboratory of Myeloid Cell Immunology, VIB Center for Inflammation Research, Brussels, Belgium. ¹¹Department of Surgery, University of South Dakota Sanford School of Medicine, Vermillion, SD, USA. ¹²ISA Pharmaceuticals, Leiden, The Netherlands. ¹³Department of Cell and Gene Therapy, Baylor College of Medicine, Houston, TX, USA.

Received: 4 November 2018 Accepted: 13 December 2018

Published online: 15 January 2019

References

1. Ferlay J, Shin HR, Bray F, Forman D, Mathers C, Parkin DM. Estimates of worldwide burden of cancer in 2008: GLOBOCAN 2008. *Int J Cancer*. 2010; 127(12):2893–917.
2. Marur S, D'Souza G, Westra WH, Forastiere AA. HPV-associated head and neck cancer: a virus-related cancer epidemic. *Lancet Oncol*. Aug. 2010;11(8):781–9.
3. Ndiaye C, Mena M, Alemany L, Arbyn M, Castellsagué X, Laporte L, Bosch FX, de Sanjosé S, Trottier H. HPV DNA, E6/E7 mRNA, and p16INK4a detection in head and neck cancers: a systematic review and meta-analysis. *Lancet Oncol*. 2014;15(12):1319–31.
4. Bontkes HJ, de Gruijl TD, van den Muysenberg AJC, Verheijen RHM, Stukart MJ, Meijer CJLM, Scheper RJ, Stacey SN, Duggan-Keen MF, Stern PL, Man S, Borysiewicz LK, Walboomers JMM. Human papillomavirus type 16 E6/E7-specific cytotoxic T lymphocytes in women with cervical neoplasia. *Int J Cancer*. 2000;88(1):92–8.
5. Lassen P, Eriksen JG, Hamilton-Dutoit S, Tramm T, Alsner J, Overgaard J. Effect of HPV-associated p16INK4A expression on response to radiotherapy and survival in squamous cell carcinoma of the head and neck. *J Clin Oncol*. 2009;27(12):1992–8.
6. Spanos WC, Nowicki P, Lee D, et al. Immune response during therapy with cisplatin or radiation for human papillomavirus-related head and neck cancer. *Arch Otolaryngol Neck Surg*. 2009;135(11):1137–46.
7. S. Braunstein and J. L. Nakamura, "Radiotherapy-induced malignancies : review of clinical features, pathobiology, and evolving approaches for mitigating risk," *Front. Oncol*, vol. 3, no. April, pp. 1–15, 2013.
8. Huang SH, Perez-Ordóñez B, Weinreb I, Hope A, Massey C, Waldron JN, Kim J, Bayley AJ, Cummings B, John Cho BC, Ringash J, Dawson LA, Siu LL, Chen E, Irish J, Gullane P, Hui A, Liu FF, Shen X, Xu W, O'Sullivan B. Natural course of distant metastases following radiotherapy or chemoradiotherapy in HPV-related oropharyngeal cancer. *Oral Oncol*. 2013;49(1):79–85.
9. Sridharan V, Margalit DN, Lynch SA, Severgnini M, Zhou J, Chau NG, Rabinowitz G, Lorch JH, Hammerman PS, Hodi FS, Haddad RI, Tishler RB, Schoenfeld JD. Definitive chemoradiation alters the immunologic landscape and immune checkpoints in head and neck cancer. *Br J Cancer*. 2016;115(2):252–60.
10. Burnette BC, Liang H, Lee Y, Chlewicki L, Khodarev NN, Weichselbaum RR, Fu Y-X, Auh SL. The efficacy of radiotherapy relies upon induction of type I interferon-dependent innate and adaptive immunity. *Cancer Res*. Apr. 2011; 71(7):2488–96.
11. Reits EA, Hodge JW, Herberts CA, Groothuis TA, Chakraborty M, Wansley EK, Camphausen K, Luiten RM, de Ru AH, Neijssen J, Griekspoor A, Mesman E, Verreck FA, Spits H, Schlom J, van Veelen P, Neefjes JJ. Radiation modulates the peptide repertoire, enhances MHC class I expression, and induces successful antitumor immunotherapy. *J Exp Med*. 2006;203(5):1259–71.
12. Schuler PJ, Harasymczuk M, Schilling B, Saze Z, Strauss L, Lang S, Johnson JT, Whiteside TL. Effects of adjuvant chemoradiotherapy on the frequency and function of regulatory T cells in patients with head and neck cancer. *Clin Cancer Res*. 2013;19(23):6585–96.
13. Al-Taei S, Banner R, Powell N, Evans M, Palaniappan N, Tabi Z, Man S. Decreased HPV-specific T cell responses and accumulation of immunosuppressive influences in oropharyngeal cancer patients following radical therapy. *Cancer Immunol Immunother*. Dec. 2013;62(12):1821–30.
14. van Meir H, Nout RA, Welters MJ, Loof NM, de Kam ML, van Ham JJ, Samuels S, Kenter GG, Cohen AF, Melief CJM, Burggraaf J, van Poelgeest MIE, van der Burg SH. Impact of (chemo) radiotherapy on immune cell composition and function in cervical cancer patients. *Oncoimmunology*. 2017;6(2):e1267095.
15. Brennan PA, Umar T, Smith GI, Lo CH, Tant S. Expression of nitric oxide synthase-2 in cutaneous squamous cell carcinoma of the head and neck. *Br J Oral Maxillofac Surg*. 2002;40(3):191–4.
16. Jacamo R, Hoang N-M, Al Rawi A, Ly C, Parihar R, McQueen T, Ruvolo PP, Williams P, Alatrash G, Konopleva M, Andreeff M. Up-Regulation of iNOS in AML Blasts Creates an Immunosuppressive Microenvironment, Inhibits T-Cell Proliferation and Transforms T-Cells Towards a Tumor-Tolerating Phenotype. *Blood*. 2017;130(Suppl 1):2443 LP-2443.
17. Jayaraman P, Parikh F, Lopez-Rivera E, Hailemichael Y, Clark A, Ma G, Cannan D, Ramacher M, Kato M, Overwijk WW, Chen SH, Umansky VV, Sikora AG. Tumor-expressed inducible nitric oxide synthase controls induction of functional myeloid-derived suppressor cells through

- modulation of vascular endothelial growth factor release. *J Immunol.* 2012;188(11):5365–76.
18. Moore WM, Webber RK, Jerome GM, Tjoeng FS, Misko TP, Currie MG. L-N6-(1-Iminoethyl)lysine: a selective inhibitor of inducible nitric oxide synthase. *J Med Chem.* 1994;37(23):3886–8.
 19. Hansel TT, Kharitonov SA, Donnelly LE, Erin EM, Currie MG, Moore WM, Manning PT, Recker DP, Barnes PJ. A selective inhibitor of inducible nitric oxide synthase inhibits exhaled breath nitric oxide in healthy volunteers and asthmatics. *FASEB J.* Jul. 2003;17(10):1298–300.
 20. Jayaraman P, Alfarano MG, Svider PF, Parikh F, Lu G, Kidwai S, Xiong H, Sikora AG. iNOS expression in CD4+ T cells limits treg induction by repressing TGFβ1: combined iNOS inhibition and treg depletion unmask endogenous antitumor immunity. *Clin Cancer Res.* 2014;20(24):6439–51.
 21. Awwad M, North RJ. Cyclophosphamide-induced immunologically mediated regression of a cyclophosphamide-resistant murine tumor: a consequence of eliminating precursor L3T4+ suppressor T-cells. *Cancer Res.* 1989;49(7):1649–54.
 22. Rahir G, Wathelet N, Hanoteau A, Henin C, Oldenhove G, Galuppo A, Lanaya H, Colau D, Mackay CR, Van Den Eynde B, Moser M. Cyclophosphamide treatment induces rejection of established P815 mastocytoma by enhancing CD4 priming and intratumoral infiltration of P1E/H-2Kd-specific CD8+ T cells. *Int J Cancer.* 2014;134(12):2841–52.
 23. Hanoteau A, Henin C, Svec D, Bisilliat Donnet C, Denanglaire S, Colau D, Romero P, Leo O, Van den Eynde B, Moser M. Cyclophosphamide treatment regulates the balance of functional/exhausted tumor-specific CD8+T cells. *Oncimmunology.* 2017;6(8).
 24. Scurr M, Pembroke T, Bloom A, Roberts D, Thomson A, Smart K, Bridgeman H, Adams R, Brewster A, Jones R, Gwynne S, Blount D, Harrop R, Hills R, Gallimore A, Godkin A. Low-dose cyclophosphamide induces antitumor T-cell responses, which associate with survival in metastatic colorectal cancer. *Clin Cancer Res.* 2017;23(22):6771–80.
 25. Vermeer DW, Coppock JD, Zeng E, Lee KM, Spanos WC, Onken MD, Uppaluri R, Lee JH, Vermeer PD. Metastatic model of HPV+ oropharyngeal squamous cell carcinoma demonstrates heterogeneity in tumor metastasis. *Oncotarget.* 2016;7(17).
 26. Spanos WC, Nowicki P, Lee DW, Hoover A, Hostager B, Gupta A, Anderson ME, Lee JH. Immune response during therapy with cisplatin or radiation for human papillomavirus-related head and neck cancer. *Arch Otolaryngol Head Neck Surg.* 2009;135(11):1137–46.
 27. Chung MK, Jung YH, Lee JK, Cho SY, Murillo-Sauca O, Uppaluri R, Shin JH, Sunwoo JB. CD271 Confers an Invasive and Metastatic Phenotype of Head and Neck Squamous Cell Carcinoma through the Upregulation of Slug. *Clin Cancer Res.* 2018;24(3):674 LP-683.
 28. Welters MJ, Ma W, Santegoets SJ, Goedemans R, Ehsan I, Jordanova ES, Van Ham VJ, Van Unen V, Koning F, Van Egmond SI, Charoentong P, Trajanoski Z, Van Der Velden LA, Van Der Burg SH. Intratumoral HPV16-specific T cells constitute a type I-oriented tumor microenvironment to improve survival in HPV16-driven oropharyngeal cancer. *Clin Cancer Res.* 2017;24(3):634–47.
 29. Santegoets SJ, van Ham VJ, Ehsan I, Charoentong P, Duurland CL, van Unen V, Höllt T, van der Velden L-A, van Egmond SI, Kortekaas K, de Vos van Steenwijk PJ, van Poelgeest MI, Welters MJ, van der Burg SH. The anatomical location shapes the immune infiltrate in tumors of same etiology and impacts survival. *Clin. Cancer Res.* 2018;2018:clinres.1749.
 30. Newton JM, Hanoteau A, Sikora AG. Enrichment and Characterization of the Tumor Immune and Non-immune Microenvironments in Established Subcutaneous Murine Tumors. *J Vis Exp.* 2018;136. <https://doi.org/10.37971/57685>.
 31. Gartrell RD, Marks DK, Hart TD, Li G, Davari DR, Wu A, Blake Z, Lu Y, Askin KN, Monod A, Esancy CL, Stack EC, Jia DT, Armenta PM, Fu Y, Izaki D, Taback B, Rabadan R, Kaufman HL, Drake CG, Horst BA, Saenger YM. Quantitative Analysis of Immune Infiltrates in Primary Melanoma. *Cancer Immunol Res.* 2018;6(4):481–93.
 32. Kitamura T, Doughty-Shenton D, Cassetta L, Fragkogianni S, Brownlie D, Kato Y, Carragher N, Pollard JW. Monocytes differentiate to immune suppressive precursors of metastasis-associated macrophages in mouse models of metastatic breast cancer. *Front Immunol.* 2018;8:2004.
 33. Balermppas P, Rödel F, Liberz R, Oppermann J, Wagenblast J, Ghanaati S, Harter PN, Mittelbronn M, Weiss C, Rödel C, Fokas E. Head and neck cancer relapse after chemoradiotherapy correlates with CD163+ macrophages in primary tumour and CD11b+ myeloid cells in recurrences. *Br J Cancer.* 2014;111(8):1509–18.
 34. Antonia SJ, Villegas A, Daniel D, Vicente D, Murakami S, Hui R, Yokoi T, Chiappori A, Lee KH, de Wit M, Cho BC, Bourhaba M, Quantin X, Tokito T, Mekhail T, Planchard D, Kim Y-C, Karapetis CS, Hiet S, Ostoros G, Kubota K, Gray JE, Paz-Ares L, de Castro Carpeño J, Wadsworth C, Melillo G, Jiang H, Huang Y, Dennis PA, Özgüroğlu M. Durvalumab after Chemoradiotherapy in Stage III Non-Small-Cell Lung Cancer. *N Engl J Med.* 2017;377:1919-1929.
 35. Hughes E, Scurr M, Campbell E, Jones E, Godkin A, Gallimore A. T-cell modulation by cyclophosphamide for tumour therapy. *Immunology.* 2018;154(1):62–8.
 36. Chalivendra V, Kanchi KL, Onken MD, Winkler AE, Mardis E, Uppaluri R. Genomic analysis to define molecular basis of aggressiveness in a mouse model of oral cancer. *Genomics Data.* 2015;3:61–2.
 37. Movahedi K, Laoui D, Gysemans C, Baeten M, Stangé G, Van den Bossche J, Mack M, Pipeleers D, In't Veld P, De Baetselier P, Van Ginderachter JA. Different Tumor Microenvironments Contain Functionally Distinct Subsets of Macrophages Derived from Ly6C(high) Monocytes. *Cancer Res.* 2010;70(14): 5728 LP-5739.
 38. Acuff NV, Linden J. Using visualization of t-distributed stochastic neighbor embedding to identify immune cell subsets in mouse tumors. *J Immunol.* Mar. 2017;198(11):4539–46.
 39. S. Kuhn, J. Yang, and F. Ronchese, "Monocyte-derived dendritic cells are essential for CD8+ T cell activation and antitumor responses after local immunotherapy," *Front Immunol.*, vol. 6, no. NOV, pp. 1–14, 2015.
 40. Engblom C, Pfirschke C, Pittet MJ. The role of myeloid cells in cancer therapies. *Nat Rev Cancer.* 2016;16(7):447–62.
 41. L. Apetoh, M. J. Smyth, C. G. Drake, J.-P. Abastado, R. N. Apte, M. Ayyoub, J.-Y. Blay, M. Bonneville, L. H. Butterfield, A. Caignard, C. Castelli, F. Cavallo, E. Celis, L. Chen, M. P. Colombo, B. Comin-Anduix, G. Coukos, M. V. Dhodapkar, G. Dranoff, I. H. Frazer, W.-H. Fridman, D. I. Gabrilovich, E. Gilboa, S. Gnjatic, D. Jäger, P. Kalinski, H. L. Kaufman, R. Kiessling, J. Kirkwood, A. Knuth, R. Liblau, M. T. Lotze, E. Lugli, F. Marincola, I. Melero, C. J. Melief, T. R. Mempel, E. A. Mittendorf, K. Odun, W. W. Overwijk, A. K. Palucka, G. Parmiani, A. Ribas, P. Romero, R. D. Schreiber, G. Schuler, P. K. Srivastava, E. Tartour, D. Valmori, S. H. van der Burg, P. van der Bruggen, B. J. van den Eynde, E. Wang, W. Zou, T. L. Whiteside, D. E. Speiser, D. M. Pardoll, N. P. Restifo, and A. C. Anderson, "Consensus nomenclature for CD8+ T cell phenotypes in cancer," *Oncimmunology*, vol. 4, no. 4, p. e998538, Apr. 2015.
 42. Herndler-Brandstetter D, Ishigame H, Shinnakasu R, Plajer V, Stecher C, Zhao J, Lietzenmayer M, Kroehling L, Takumi A, Kometani K, Inoue T, Kluger Y, Kaech SM, Kurosaki T, Okada T, Flavell RA. KLRG1+Effector CD8+T Cells Lose KLRG1, Differentiate into All Memory T Cell Lineages, and Convey Enhanced Protective Immunity. *Immunity.* 2018;48(4):716–729.e8.
 43. Meiraz A, Garber OG, Harari S, Hassin D, Berke G. Switch from perforin-expressing to perforin-deficient CD8+ T cells accounts for two distinct types of effector cytotoxic T lymphocytes in vivo. *Immunology.* 2009;128(1):69–82.
 44. Lu SL, Reh D, Li AG, Woods J, Corless CL, Kulesz-Martin M, Wang XJ. Overexpression of transforming growth factor β1 in head and neck epithelia results in inflammation, angiogenesis, and epithelial hyperproliferation. *Cancer Res.* 2004;64(13):4405–10.
 45. Lathers DM, Young MRL. Increased aberrance of cytokine expression in plasma of patients with more advanced squamous cell carcinoma of the head and neck. *Cytokine.* Mar. 2004;25(5):220–8.
 46. Uyttenhove C, Pilotte L, Théate I, Stroobant V, Colau D, Parmentier N, Boon T, Van den Eynde BJ. Evidence for a tumoral immune resistance mechanism based on tryptophan degradation by indoleamine 2,3-dioxygenase. *Nat Med.* Sep. 2003;9:1269.
 47. Davis RJ, Van Waes C, Allen CT. Overcoming barriers to effective immunotherapy: MDSCs, TAMs, and Tregs as mediators of the immunosuppressive microenvironment in head and neck cancer. *Oral Oncol.* 2016;58:59–70.
 48. Younis RH, Han KL, Webb TJ. Human head and neck squamous cell carcinoma-associated Semaphorin 4D induces expansion of myeloid-derived suppressor cells. *J Immunol.* 2016;196(3):1419–29.
 49. Bronte V, Serafini P, Mazzoni A, Segal DM, Zanovello P. L-arginine metabolism in myeloid cells controls T-lymphocyte functions. *Trends in Immunology.* 2003;6:302–6.
 50. Redd PS, Ibrahim ML, Klement JD, Sharman SK, Paschall AV, Yang D, Nayak-Kapoor A, Liu K. SETD1B activates iNOS expression in myeloid-derived suppressor cells. *Cancer Res.* 2017;77(11):2834–43.
 51. Serafini P, Borrello I, Bronte V. Myeloid suppressor cells in cancer: recruitment, phenotype, properties, and mechanisms of immune suppression. *Semin Cancer Biol.* 2006;16(1):53–65.

52. Matsunaga T, Yamaji Y, Tomokuni T, Morita H, Morikawa Y, Suzuki A, Yonezawa A, Endo S, Ikari A, Iguchi K, El-Kabbani O, Tajima K, Hara A. Nitric oxide confers cisplatin resistance in human lung cancer cells through upregulation of aldo-keto reductase 1B10 and proteasome. *Free Radic Res*. Nov. 2014;48(11):1371–85.
53. Saleem W, Suzuki Y, Mobaraki A, Yoshida Y, Noda S, Saitoh JJ, Nakano T. Reduction of nitric oxide level enhances the radiosensitivity of hypoxic non-small cell lung cancer. *Cancer Sci*. 2011;102(12):2150–6.
54. Battaglia A, Buzzonetti A, Martinelli E, Fanelli M, Petrillo M, Ferrandina G, Scambia G, Fattorossi A. Selective changes in the immune profile of tumor-draining lymph nodes after different neoadjuvant Chemoradiation regimens for locally advanced cervical Cancer. *Int J Radiat Oncol Biol Phys*. 2010;76(5):1546–53.
55. Frey B, Rückert M, Weber J, Mayr X, Derer A, Lotter M, Bert C, Rödel F, Fietkau R, Gaipl US. Hypofractionated irradiation has immune stimulatory potential and induces a timely restricted infiltration of immune cells in Colon Cancer tumors. *Front Immunol*. 2017;8:231.
56. Hettich M, Lahoti J, Prasad S, Niedermann G. Checkpoint Antibodies but not T Cell-Recruiting Diabodies Effectively Synergize with TIL-Inducing γ -Irradiation. *Cancer Res*. 2016;76(16):4673 LP-4683.
57. Crocenzi T, Cottam B, Newell P, Wolf RF, Hansen PD, Hammill C, Solhjem MC, To YY, Greathouse A, Tormoen G, Jutric Z, Young K, Bahjat KS, Gough MJ, Crittenden MR. A hypofractionated radiation regimen avoids the lymphopenia associated with neoadjuvant chemoradiation therapy of borderline resectable and locally advanced pancreatic adenocarcinoma. *J Immunother Cancer*. 2016;4(1):1–13.
58. Zhang T, Yu H, Ni C, Zhang T, Liu L, Lv Q, Zhang Z, Wang Z, Wu D, Wu P, Chen G, Wang L, Wei Q, Huang J, Wang X. Hypofractionated stereotactic radiation therapy activates the peripheral immune response in operable stage I non-small-cell lung cancer. *Sci Rep*. 2017;7(1):1–10.
59. Mok S, Duffy CR, Allison JP. Abstract 2984: Effects of anti-CTLA-4 and anti-PD-1 on memory T-cell differentiation and resistance to tumor relapse. *Cancer Res*. 2018;78(13 Supplement):2984 LP-2984.
60. Welters MJ, van der Sluis TC, van Meir H, Loof NM, van Ham VJ, van Duikeren S, Santegoets SJ, Arens R, de Kam ML, Cohen AF, van Poelgeest MI, Kenter GG, Kroep JR, Burggraaf J, Melief CJ, van der Burg SH. Vaccination during myeloid cell depletion by cancer chemotherapy fosters robust T cell responses. *Sci Transl Med*. 2016;8(334):334ra52.
61. Abu Eid R, Razavi GSE, Mkrtychyan M, Janik J, Khleif SN. Old-School Chemotherapy in Immunotherapeutic Combination in Cancer, A Low-cost Drug Repurposed. *Cancer Immunol Res*. 2016;4(5):377 LP-382.
62. Ghiringhelli F, Menard C, Puig PE, Ladoire S, Roux S, Martin F, Le Cesne A, Zitvogel L, Chauffert B. Metronomic cyclophosphamide regimen selectively depletes CD4+CD25+ regulatory T cells and restores T and NK effector functions in end stage cancer patients. *Cancer Immunol Immunother*. 2007;56(5):641–8.
63. Ge Y, Domschke C, Stoiber N, Schott S, Heil J, Rom J, Blumenstein M, Thum J, Sohn C, Schneeweiss A, Beckhove P, Schuetz F. Metronomic cyclophosphamide treatment in metastasized breast cancer patients: immunological effects and clinical outcome. *Cancer Immunol Immunother*. 2012;61(3):353–62.
64. Machiels J-PH, Reilly RT, Emens LA, Ercolini AM, Lei RY, Weintraub D, Okoye FI, Jaffee EM. Cyclophosphamide, Doxorubicin, and Paclitaxel Enhance the Antitumor Immune Response of Granulocyte/Macrophage-Colony Stimulating Factor-secreting Whole-Cell Vaccines in HER-2/neu Tolerized Mice. *Cancer Res*. 2001;61(9):3689 LP-3697.
65. Serafini P, Meckel K, Kelso M, Noonan K, Califano J, Koch W, Dolcetti L, Bronte V, Borrello I. Phosphodiesterase-5 inhibition augments endogenous antitumor immunity by reducing myeloid-derived suppressor cell function. *J Exp Med*. 2006;203(12):2691 LP-2702.
66. Weed DT, Vella JL, Reis IM, De la fuente AC, Gomez C, Sargi Z, Nazarian R, Califano J, Borrello I, Serafini P. Tadalafil Reduces Myeloid-Derived Suppressor Cells and Regulatory T Cells and Promotes Tumor Immunity in Patients with Head and Neck Squamous Cell Carcinoma. *Clin Cancer Res*. 2015;21(1):39 LP-48.
67. Hoyt JC, Ballering J, Numanami H, Hayden JM, Robbins RA. Doxycycline Modulates Nitric Oxide Production in Murine Lung Epithelial Cells. *J Immunol*. 2006;176(1):567 LP-572.
68. Ritchie ME, Phipson B, Wu D, Hu Y, Law CW, Shi W, Smyth GK. Limma powers differential expression analyses for RNA-sequencing and microarray studies. *Nucleic Acids Res*. 2015;43:e47.
69. Barbie DA, Tamayo P, Boehm JS, Kim SY, Moody SE, Dunn IF, Schinzel AC, Sandy P, Meylan E, Scholl C, Fröhling S, Chan EM, Sos ML, Michel K, Mermel C, Silver SJ, Weir BA, Reiling JH, Sheng Q, Gupta PB, Wadlow RC, Le H, Hoersch S, Wittner BS, Ramaswamy S, Livingston DM, Sabatini DM, Meyerson M, Thomas RK, Lander ES, Mesirov JP, Root DE, Gilliland DG, Jacks T, Hahn WC. Systematic RNA interference reveals that oncogenic KRAS-driven cancers require TBK1. *Nature*. 2009;462:108-12.
70. Hänzelmann S, Castelo R, Guinney J. GSEA: gene set variation analysis for microarray and RNA-Seq data. *BMC Bioinformatics*. 2013;14:7.

Ready to submit your research? Choose BMC and benefit from:

- fast, convenient online submission
- thorough peer review by experienced researchers in your field
- rapid publication on acceptance
- support for research data, including large and complex data types
- gold Open Access which fosters wider collaboration and increased citations
- maximum visibility for your research: over 100M website views per year

At BMC, research is always in progress.

Learn more biomedcentral.com/submissions

